GENETIC ANALYSIS IN THREE INHERITED DISORDERS

by

Tarık Bozoğlu

B.S., Molecular Biology and Bioengineering, Sabancı University, 2005

Submitted to the Institute for Graduate Studies in
Science and Engineering in partial fulfillment of
the requirements for the degree of
Master of Science

Graduate Program in Molecular Biology and Genetics

Boğaziçi University

2008

ACKNOWLEDGMENTS

Completing this study was possible only by my supervisor Dr. Aslı Tolun's superb skills as a mentor and tutor. I treasure her most valuable guidance and patience.

I would like to thank Dr. Sibel Uğur İşeri, for all the knowledge she has generously shared.

I wish to acknowledge the patience Murat Çetinkaya has showed as he assisted my orientation to the lab.

I thank my fellow lab members for spreading their joy to create a delightful atmosphere.

I owe everything to my family, for supporting me all the way.

for her and her…

ABSTRACT

GENETIC ANALYSIS IN THREE INHERITED DISORDERS

Genes responsible for inherited disorders can be localized on the genome by genetic linkage analysis. Mapping of a disease locus is accomplished by genotyping the family members with polymorphic markers in order to identify crossovers and observe allele segregation with the disease. Initially, a whole-genome scan is conducted to identify genotypes. Possible loci are determined using linkage programs and then further investigated by fine-mapping using densely spaced markers. After finding the disease locus, candidate gene approach is applied to identify the causative defect and thus the gene responsible for the disease.

In this study genetic investigation was performed on three hereditary diseases. Focal dermal hypoplasia (FDH) commonly manifests with dermal, skeletal, ocular, oral and soft tissue abnormalities. X-linked inheritance of the disorder allowed omitting the genome scan in favor of a dense mapping of the X chromosome. The locus found was narrowed down by fine mapping. The number of genes residing at the identified gene locus was too large to allow a simple search for the disease gene. At that time, a gene at the locus, *PORCN,* was reported to be the disease gene, so it was screened for mutations in the family studied. No mutation was found; however, gene expression in patients was found reduced.

Autosomal recessive microhydranencephaly (MHAC) is congenital and refers to the rare co-occurrence of microcephaly and hydranencephaly, with gene locus at chromosome 16p13.13-p12.2. We applied candidate gene approach and analyzed three genes at the locus and found a deletion (c.1-3548_83+644del) in *NDE1*.

Frequent occurrence of brain tumors was observed in a non-consanguineous family, indicating familial inheritance. Genetic linkage analysis performed related the condition to

a locus; however, the results were inconclusive as the penetrance value of the condition was unascertainable.

ÖZET

ÜÇ KALITSAL HASTALIKTA GENETİK İNCELEME

Kalıtsal bir hastalıktan sorumlu genin genomdaki yeri genetik bağlantı analizi ile saptanabilir. Bu amaç için, önce alellerin hastalıkla ayrışımını ve çapraz-atlamaları belirlemek amacıyla aile fertleri polimorfik belirteçler kullanarak genotiplenir. Genotipleme sonuçları kullanılarak da hastalık lokusu haritalanır. Bu bağlamda, öncelikle genom çapında bir tarama ile aleller belirlenir. Bağlantı programları kullanılarak olası lokuslar saptanır ve sık aralıklı belirteçler ile irdelenir. Hastalık lokusunun bulunmasından sonra, aday gen yaklaşımı ile hastalığa yol açan gen kusuru ve dolayısıyla hastalıktan sorumlu gen bulunur.

Bu çalışmada üç kalıtsal hastalık üzerine genetik inceleme gerçekleştirildi. Fokal dermal hipoplasi (FDH) deri, iskelet, göz, ağız ve yumuşak doku bozuklukları gösterir. X-kromozomu geçişli olması nedeniyle, tüm genom taraması gerekmedi ve yalnızca X-kromozomunun taranması yeterli oldu. Bulunan gen lokusu ince haritalanarak daraltıldı. Bu lokusta aday gen yaklaşımı için çok fazla gen bulunuyordu. Bu sırada, genlerden birinin, PORCN, FDH'a sebep olduğu rapor edildi. Gen ailede taranarak mutasyon arandı. Bir mutasyon bulunamadı, fakat hastalarda gen anlatımının düşük olduğu belirlendi.

Otozomal çekinik mikrohidranensefalide (MHAC), mikrosefali ve hidranensefalinin nadir birlikteliği doğuştan görülür. Hastalık geni 16p13.13-p12.2 lokusuna haritalanmıştır. Aday gen yaklaşımı ile lokustaki genlerden üçü incelendi ve NDE1 geninde delesyon (c.1-3548_83+644del) bulundu.

Akraba evliliği olmayan bir ailede beyin tümörlerinin sık görülmesi tümör oluşumuna ailesel yatkınlığı düşündürdü. Genetik bağlantı analizi sonucunda hastalık bir lokusla ilişkilendirildi, ama penetrans değerinin belirlenemez oluşu nedeniyle kesin bir sonuç elde edilemedi.

TABLE OF CONTENTS

LIST OF FIGURES

LIST OF TABLES

LIST OF SYMBOLS / ABBREVIATIONS

A	Adenine
C	Cytosine
G	Guanine
T	Thymine
ASPM	Abnormal Spindle-Like, Microcephaly Associated
BRCA2	Breast Cancer 2
bp	Base Pair
C16ORF63	Chromosome 16 Open Reading Frame 63
CACNG3	Voltage-Dependent Calcium Channel Gamma Subunit 3
CDK5RAP2	CDK5 Regulatory Subunit Associated Protein 2
cDNA	Complementary Deoxyribonucleic Acid
CDR2	Cerebellar Degeneration-Related Protein 2
CENPJ	Centromere Protein J
CIAO1	Cytosolic Iron-Sulfur Protein Assembly 1 Homolog
cM	Centi Morgan
CpG	Cytosine-Phosphate-Guanine
CRYM	Crystallin, Mu
DNA	Deoxyribonucleic Acid
EGFR	Epidermal Growth Factor Receptor
FDH	Focal Dermal Hypoplasia
GAC1	Glioma Amplified on Chromosome 1
GAS41	Glioma-Amplified Sequence-41
GFER	Growth Factor, Augmenter of Liver Regeneration
GLI	Glioma-Associated Oncogene Homolog 1
GLTSCR1	Glioma Tumor Suppressor Candidate Region Gene 1
GLTSCR2	Glioma Tumor Suppressor Candidate Region Gene 2
GRIN2A	Glutamate Receptor, Ionotropic, N-Methyl D-Aspartate 2A
GSPT1	G1 to S Phase Transition 1
GTP	Guanosine Triphosphate

HBT	Hereditary Brain Tumors
kb	Kilobase
LGI1	Leucine-Rich, Glioma Inactivated 1
Lod	Logarithm of Odds
Mb	Megabase
MHAC	Microhydranencephaly
min	Minute
MN1	Meningioma 1
N/A	Not Available
NCBI	National Center For Biotechnology Information
NDE1	Nuclear Distribution Gene E Homolog 1
NF2	Neurofibromin 2
OMIM	Online Mendelian Inheritance in Man
PAGE	Polyacrylamide Gel Electrophoresis
PCR	Polymerase Chain Reaction
PLK1	Polo-Like Kinase 1
pLOD	Parametric Lod Score
PORCN	Porcupine Homolog
PPARG	Peroxisome Proliferator-Activated Receptor Gamma
PTEN	Phosphatase and Tensin Homolog
qPCR	Quantitative Polymerase Chain Reaction
SDS	Sodium Dodecyl Sulphate
SNP	Single Nucleotide Polymorphism
SOCS1	Suppressor of Cytokine Signaling 1
SSCP	Single Strand Conformational Polymorphism
TEMED	N, N, N, N'-Tetramethylethylenediamine
UTR	Untranslated Region
WNT	Wingless-Type MMTV Integration Site Family Member

1. INTRODUCTION

In this study, genetic analysis was performed in three inherited disorders aiming for gene localization, linkage investigation, or disease gene identification. Four afflicted families were available for investigation of focal dermal hypoplasia, microhydranencephaly and hereditary brain tumors.

1.1. Focal Dermal Hypoplasia

Focal dermal hypoplasia (FDH, OMIM 305600) is a hereditary disease commonly manifesting with dermal, skeletal, ocular, oral and soft tissue abnormalities. Also called Goltz syndrome, it was first described in 1962, in a family of four generations of affected females (Goltz *et al.,* 1962). The majority of FDH cases are caused by *de novo* mutations (95 per cent of female cases and all male cases), with 90 percent of all cases being females (Goltz, 1992). There are several reports of male-to-female transmissions of FDH, but no male-to-male transmission has been reported. These findings led to the hypothesis that FDH has an X-linked dominant inheritance pattern with *in utero* lethality in males and that male cases are somatic mosaics, allowing transmission to daughters whenever gonads are affected (Gorski, 1991).

The commonly observed clinical symptoms in FDH patients include dermal defects such as atrophic skin, linear pigmentation of skin, fat herniation through the dermal defects, and multiple papillomas of skin; oral anomalies such as lip papillomas and hypoplastic teeth; ocular anomalies such as coloboma of iris and choroid, strabismus and microphthalmia; skeletal anomalies such as striated bones, digital anomalies of syndactyly, polydactyly, camptodactyly, and absence deformities; and mental retardation.

In this study, a family presenting three generations of female FDH cases were subjected to genetic analysis. Three of the patients (proband in the 3rd generation, her mother and her maternal grandmother; Figure 3.1) have been described (Seven *et al.,* 1998). Family history revealed that several other members had skin lesions similar to the proband. All cases were female, and an increased rate of miscarriages was reported.

Linkage analysis in X-chromosome was performed with the purpose of determining the disease locus and subsequently identifying the underlying molecular defect.

1.2. Microhydranencephaly

Familial autosomal recessive microhydranencephaly (MHAC; OMIM 605013) was first described in a large inbred Anatolian family (Kavaslar *et al.,* 2000). All three patients in this family were born to first cousin marriages. Patients displayed a rare combination of hydranencephaly and microcephaly. Hydranencephaly is a neural tube development defect, causing cerebral dysplasia and replacement of cerebral tissues with spinocerebellar fluid. The syndrome is usually attributed to exogenous causes. Microcephaly is a condition defined by a small head circumference, more than three standard deviations below the average of sex and age of the patient. Association of these two conditions together with familial inheritance led to defining the disease as novel. Manifestations of the disease also included a very small body, limited motor and communicative abilities, spastic quadriplegia, multiple joint contractures, bilateral pes equina varus, myoclonic seizures, and athetosis. The disease was mapped to chromosome 16p13.13-p12.2 by autozygosity mapping.

Other familial cases with phenotypic similarity to MHAC were later reported. Three sibships presented in two reports shared microcephaly and psychomotor retardation, and neural tube development defects (Alexander *et al.,* 1995, Schram *et al*, 2004). No linkage information is available for those cases. Also, external insults during development were not ruled out. Recently two Slovak brothers in a non-consanguineous family with similar findings were diagnosed with MHAC (Behunova *et al.,* submitted).

Linkage of MHAC to chromosome 16 presented the opportunity to identify the gene responsible. Previously several candidate genes had been selected by the criteria of affecting neural tube development and screened for mutations in patients: *CACNG3*, *GFER*, *GSPT1* and *CIAO1*. Of those, *GFER* and *CIAO1* no longer map to MHAC locus, as they did when the screening studies were conducted. No mutation was found in any of the genes. In addition, other candidates (*CDR2*, *CRYM*, and *GRIN2A*) were suggested but not analyzed (Tura, 2001).

Further refining of the MHAC locus and determining the gene responsible for the syndrome were attempted in this study. Genetic linkage was performed in Slovak family mentioned above, along with the continuation of candidate gene approach with new selection criteria using recent genetic information regarding related syndromes.

1.3. Hereditary Brain Tumors

Several individuals in a non-consanguineous Turkish family of three generations were diagnosed with brain tumors. Characterization of tumors revealed the diversity in types, being either astrocytomas or meningiomas. Observation of five cases in two generations suggested hereditary susceptibility or incomplete dominant inheritance, which justified the investigation by linkage analysis. Thus, a locus was searched for a putative gene responsible for hereditary brain tumors (HBT).

Gliomas (OMIM 137800) and meningiomas (OMIM 607174) are neoplasms of the central nervous system. Meningiomas are commonly benign tumors developing from arachnoidal cap cells. Their occurrence is mainly sporadic, yet familial cases have been reported. Most of the familial meningiomas are associated with neurofibromatosis type II. Investigation of meningiomas revealed mutations in *PTEN* (10q23.31; Staal *et al.,* 2002), *MN1* (22q12.3-qter; Lekanne Deprez *et al.,* 1995) and *NF2* (22q12.2; Wellenreuther *et al.,* 1995).

Glioblastoma multiforme is an aggressive type of brain tumor. Several familial cases have been described as autosomal recessive or multifactorial (Malmer *et al.,* 2001, de Andrade *et al.,* 2001). Genetic analysis for gliomas revealed defects in several genes including *GAC1* (1q32.1; Almeida *et al.,* 1998), *PPARG* (3p25; Zhou *et al.,* 2000), *EGFR* (7p12.3-p12.1; Henn *et al.,* 1986), *LGI1* (10q24; Chernova *et al.,* 1998), *PTEN* (10q23.31; Staal *et al.,* 2002), *GLTSCR1* and *GLTSCR2* (19q13.3; Smith *et al.,* 2000), *GAS41* (12q13-q15; Fischer *et al.,* 1997), *GLI* (12q13.2-13.3; Kinzler *et al.,* 1987), *BRCA2* (13q12.3; Reid *et al.,* 2005).

1.4. Linkage Analysis

Genetic linkage of two loci is a result of their proximity affecting the probability their coinheritance. The probability of a homologous recombination occurring between two loci during meiosis is inversely proportional to the distance between the loci. Under no linkage, two loci are independently assorted; probability of recombination (recombination fraction) is 0.5. The use of a series of closely positioned polymorphic chromosomal markers such as microsatellites allows detecting recombination events during meioses. This information can be utilized to locate a disease gene on the genome by determining the regions co-inherited exclusively with the disease.

In this study, microsatellite repeats were used as markers, although single nucleotide polymorphisms (SNP) are also commonly used as markers. Genotypes generated at such polymorphic markers are used to calculate logarithm of odds (LOD) scores. A lod score is the decimal logarithm of odds ratio, which is a function of the recombination fraction. Odds ratio is the ratio of the probability of the distribution of two traits in a pedigree occurring with linkage at a specified recombination fraction to the probability of observing the same distribution without linkage between the traits. Simultaneous calculation of the lod scores for more than two loci using a genetic map of markers extracts the highest possible information from linkage analysis. The complexity of such calculations requires the assistance of computer programs. Parameters such as penetrance value and disease allele frequency are required for defining the disease inheritance model. A lod score of 3 is the threshold of accepting linkage, and -2 is the threshold of exclusion. Scores in-between are inconclusive.

1.5. Candidate Gene Approach

Identification of a disease locus is a precursor for the identification of a gene defect underlying a disease. Even after mapping the locus with informative markers to a minimum region, the total number of genes residing at the locus is usually too large to analyze all genes. Therefore, a few of the genes needs to be selected for analysis. The selection criteria assess the compatibility of the disease phenotype with the gene product's known functions, structures and interactions, the expression pattern of the gene in relevant

tissues and developmental stages, and involvement of the gene in similar diseases. A solid comprehension of the disease phenotype is crucial in candidate selection, as the candidate gene must be a part of the proposed mechanism of action for the disease. The selected candidates are then screened in the patients for mutations they may be harboring.

2. PURPOSE

This study was conducted to localize by genetic linkage analysis the genes responsible and/or identify the underlying genetic defects in three inherited disorders. For focal dermal hypoplasia, mapping the disease locus using its hereditary transmission in one family and subsequent identification of the gene was aimed. Later in the study this purpose shifted to searching *PORCN* gene defects, identified meanwhile by another research group as the disease gene. MHAC studies had two purposes: investigation of genetic linkage of Slovak family to the MHAC locus in order to narrow down the known gene locus and subsequently disease gene identification. Lastly, mapping the gene for hereditary susceptibility to developing brain tumors was intended.

3. MATERIALS

3.1. Subjects

Members of four families afflicted with three different inherited diseases were available for study. The study has been approved by Boğaziçi University Committee on Research with Human Participants.

3.1.1 FDH

Members of a family of Turkish and Italian descent and afflicted with FDH were the subjects of this study (Figure 3.1). All patients were females, as is common with FDH. Three members, namely the proband (404), her mother (302) and her grand mother (203), were previously diagnosed and their clinical features described (Seven *et al.,* 1998). Affliction of several other members among the maternal relations of the proband (304, 308, 312, 402) was also indicated. Blood samples had been previously obtained from all patients and several healthy relatives, and genomic DNA extracted. Additional blood samples were later obtained from 302 and 304 for total RNA extraction.

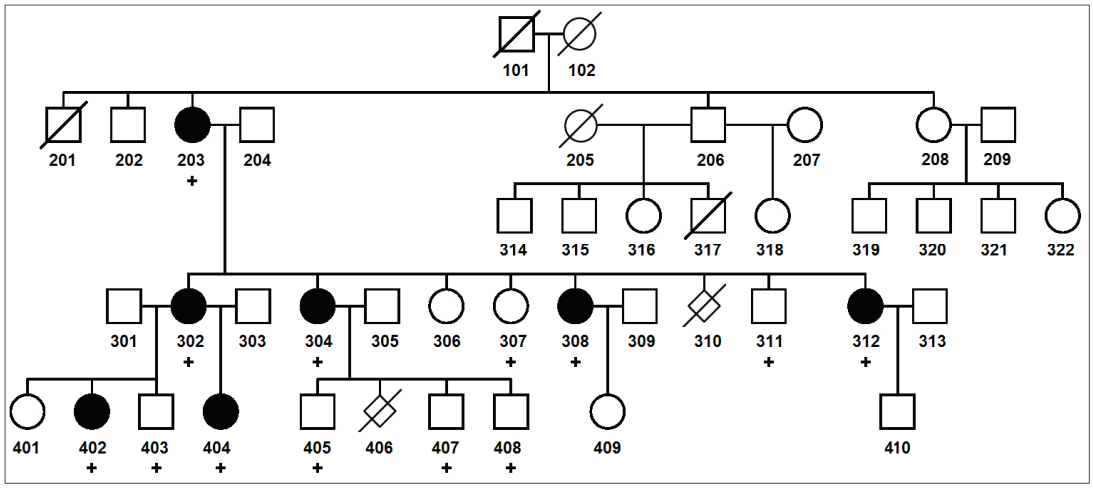

Figure 3.1. Pedigree diagram for the FDH family. DNA availability is indicated with a plus sign.

3.1.2 MHAC

MHAC phenotype was previously defined in three patients from a consanguineous Anatolian family (Kavaslar *et al.,* 2000). A similar phenotype was observed by Dr. Jana Behunova in the two siblings of a Slovak nuclear family (Figure 5.5). The parents had declared no blood relation. Dr. Behunova provided genomic DNA samples of the patients and parents for linkage analysis.

Mother of patient 1 in the Anatolian MHAC family (Figure 3.2) became pregnant. Her clinicians performed chorionic villus sampling and provided us with the fetal genomic DNA sample for genetic diagnosis. DNA samples from the parents and afflicted siblings of the fetus had been previously obtained (Kavaslar *et al.,* 2000).

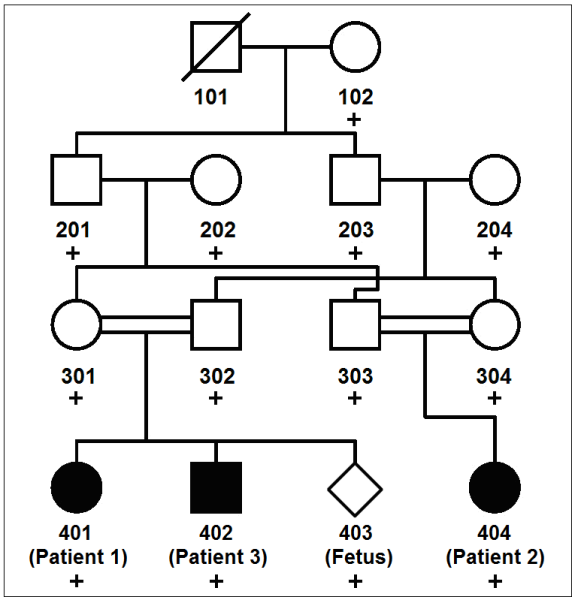

Figure 3.2. Partial pedigree diagram for the Anatolian MHAC family. DNA availability is indicated with a plus sign.

3.1.3 HBT

Five members of a Turkish family in three generations had several cases of brain tumors (Figure 3.3). Tumors were characterized as either grade IV astrocytomas (glioblastoma multiforme) or meningiomas. Tumors were observed in two siblings in the second generation (207, 209) as meningiomas and three cousins in the third generation

(301, 306, 310) as glioblastomas, indicating a familial affliction. Blood samples from most members of the family had been obtained and genomic DNA extracted previously in our laboratory.

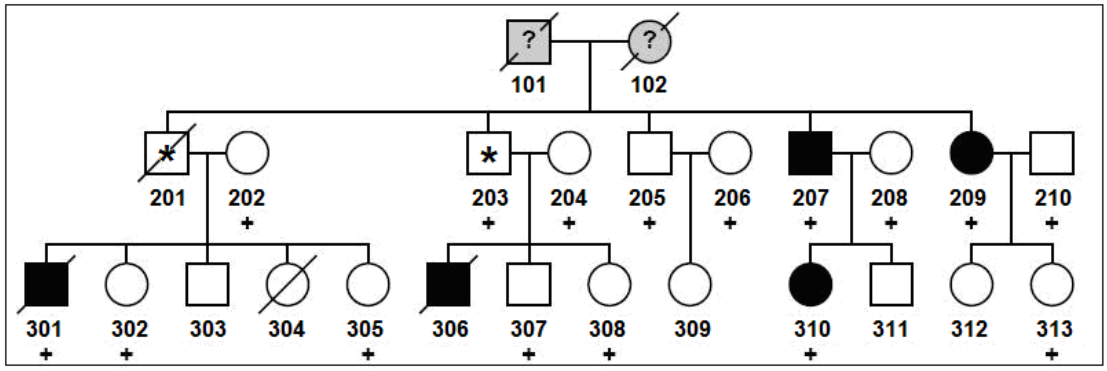

Figure 3.3. Pedigree diagram for Hereditary Brain Tumors family. DNA availability is indicated with a plus sign. Obligate carriers are indicated with asterisks.

3.2. Chemicals

All solid and liquid chemicals used in this study were purchased from Merck (Germany), Sigma (USA), Riedel de-Häen (Germany), Carlo Erba (Italy) or Biochrom (Germany) unless stated otherwise.

3.3. Buffers and Solutions

All solutions were prepared with PCR grade distilled water unless stated otherwise.

3.3.1. Polymerase Chain Reaction (PCR)

- 10 X Buffer A: 20 mM $MgCl_2$, 500 mM KCl, 100 mM Tris-HCl (pH 8.3) (Sterilized by filtering)
- 10 X Buffer B: 20 mM $MgSO_4$, 100 mM KCl, 200 mM Tris-HCl (pH 8.8), 100 mM $(NH_4)_2SO_4$, 1 per cent Triton X-100, 1 mg/ml Bovine Serum Albumin (BSA) (Sterilized by filtering)
- 5 X Combinatorial Enhancer Solution (CES): 2.7 M betaine, 6.7 mM dithiothreitol (DTT), 6.7 per cent dimethyl sulfoxide (DMSO), 55 µg/ml BSA

- $MgCl_2$: 25 mM $MgCl_2$ (Roche, Germany)
- dNTP mix: 12.5 mM each of dATP, dCTP, dGTP and dTTP (Roche, Germany)
- Betaine: 5 M Betaine (Promega, USA).

3.3.2. Agarose Gel Electrophoresis

- Agarose: 2 per cent Agarose in 0.5 X TBE buffer
- Nusieve Agarose: 2 per cent Agarose-NuSieve (2:1) in 1 X TBE buffer
- 10 X TBE Buffer: 20 mM EDTA, 0.89 M boric acid, 0.89 M Trizma base (pH 8.3)
- 6 X Loading Buffer: 10 mM Tris-HCl (pH 7.6), 50 per cent glycerol, 60 mM EDTA, 2.5 mg/ml bromophenol blue, 2.5 mg/ml xylene cyanol
- EtBr: 10 mg/ml ethidium bromide.

3.3.3. Polyacrylamide Gel Electrophoresis (PAGE)

- 40 per cent Acrylamide Stock: 40 per cent (w/v) acrylamide-bisacrylamide (19:1)
- 8 per cent Denaturing Instagel: 8 per cent acrylamide-bisacrylamide (19:1), 8.3 M urea in 1 X TBE buffer
- APS: 10 per cent (w/v) ammonium persulfate
- TEMED: N,N,N',N'-tetramethyl-ethane-1,2-diamine
- 10X Loading Buffer: 95 per cent (v/v) formamide, 20 mM EDTA, 0.05 per cent (w/v) xylene cyanol, 0.05 per cent (w/v) bromophenol blue.

3.3.4. Single Strand Conformational Polymorphism (SSCP) Analysis

- 40 per cent Acrylamide Stock: 40 per cent (w/v) acrylamide-bisacrylamide (37.5:1)
- 8 per cent Acrylamide Gel Solution: 8 per cent acrylamide-bisacrylamide (37.5:1) in 0.6 X TBE buffer
- Glycerol: 5 per cent glycerol in gel solution (Sterilized by autoclaving)

3.3.5. Silver Nitrate Staining

- Staining Buffer: 0.1 per cent $AgNO_3$
- Developing Buffer: 1.5 per cent NaOH, 0.01 per cent $NaBH_4$, 0.015 per cent formaldehyde.

3.3.6. Total RNA extraction from Blood Samples

- Cell Lysis Buffer: 155 mM NH4Cl, 10 mM KHCO3, 0.1 mM Na_2EDTA (pH 7.4) (Sterilized by autoclaving)

3.4. Fine Chemicals

3.4.1. Enzymes

Taq DNA polymerase, produced as described by Engelke *et al.,* 1990, was used in routine amplifications. For reactions requiring amplification of templates longer than 3000 bp, commercial kits were used (see section 3.4.4).

3.4.2. Oligonucleotides

Oligonuclotide primers were custom synthesized commercially in Massachusetts General Hospital (MGH) DNA Synthesis Core (USA) and sent in lyophilized form. They were later dissolved in 1 ml dH_2O and stored at -20°C.

3.4.3. Molecular Weight Markers

pUC19 DNA/*Msp*I markers were purchased from Fermentas (Lithuania) and 50 bp DNA ladder from Roche (Germany).

3.4.4. Commercial Kits

Various kits were used for special purposes:

- Qiagen Taq PCR Core Kit with Q-solution: Amplification of GC-rich templates (Qiagen, USA)
- Expand Long Range, dNTPack: Amplification of long templates (Roche, Germany)
- QIAquick PCR Purification Kit: PCR product purification (Qiagen, USA)
- REPLI-g Mini Kit: Whole genome amplification from limited amounts of genomic DNA sample (Qiagen, USA)
- RNeasy Mini Kit: RNA isolation from cells (Qiagen, USA)
- Transcriptor First Strand cDNA Synthesis Kit: Reverse Transcription of RNA samples (Roche, Germany)
- LightCycler 480 DNA SYBR Green I Master: Real time quantitative PCR (Roche, Germany).

3.5. Equipment

- Autoclave: Midas 55 (Prior Clave, UK), AMB430T (Astell, UK)
- Balance: Electronic Balance (Precisa, Switzerland)
- Centrifuges: MiniSpin Plus (Eppendorf, Germany), Universal 16R (Hettich, Germany), Allegra X-22R (Beckman Coulter, USA), J2-MC (Beckman Coulter, USA)
- Deep Freezers: -20^{o}C (Bosch, Germany), -20^{o}C (AEG, Turkey), -80^{o}C Ultra Freezer (Thermo Scientific, USA)
- Documentation System: GelDoc Documentation System with Quantity One 1-D Analysis Software (BioRad, USA)
- Electrophoretic Equipment: Horizontal DNA Electrophoresis Gel Box (Bio-Rad, USA), Primo Minicell Horizontal Gel Sytem (Thermo Scientific, USA), Sequi-Gen GT Sequencing Cell (Bio-Rad, USA), DCode Universal Mutation Detection System (Bio-Rad, USA)
- Incubator: Orbital (Gallenkamp, Germany)
- Magnetic Stirrer: MR3001 (Heidolph, Germany)
- Micropipettes: Pipetman (Gilson, France)
- Minishaker: Rotamax 120 (Heidolph, Germany)
- Ovens: Heraus (Germany), EN 400 (Nüve, Turkey)

- Power Supplies: Power Pac Model 3000 (Bio-Rad, USA), Fotoforce 250 Electrophoresis Power Supply (Fotodyne, USA), P250A Power Supply (Sigma-Aldrich, USA)
- Refrigerator: 4^{o}C (Arçelik, Turkey)
- Spectrophotometers: NanoDrop 1000 (Thermo Scientific, USA)
- Thermal Cyclers: MyCycler (Bio-Rad, USA), PTC-200 (MJ Research, USA), Techne (Progene, UK), LightCycler 480 (Roche, Germany)
- Transilluminator: Fluorescent Table (Consort, Belgium)
- Vortex: Reax vortex mixer (Heidolph, Germany), Lab Dancer Vario (Roth, Germany)
- Waterbath: Grant LTD 6G Themostatic Water Bath (Grant, Germany)
- Water Purification System: Ultra Pure Water Purification system (Watech, Germany).

3.6. Electronic Databases

- Ensembl (http://www.ensembl.org/): Reference sequence and working draft assemblies with a large collection of analytic tools
- NCBI Genome Resources (http://www.ncbi.nlm.nih.gov/genome/guide/human/): Reference sequence and working draft assemblies with a large collection of analytic tools
- Online Mendelian Inheritance in Man (http://www.ncbi.nlm.nih.gov/Omim/): A guide to human genes and inherited disorders
- UCSC Genome Browser (http://genome.ucsc.edu/): Reference sequence and working draft assemblies with a large collection of analytic tools
- Tandem Repeats Finder (http://tandem.bu.edu/trf/trf.html/): Analysis of DNA sequences for tandem repeats
- Laboratory of Statistical Genetics at Rockefeller University (http://linkage.rockefeller.edu/): A list of statistical tools for genetic linkage analysis
- Rutgers Map (http://compgen.rutgers.edu/maps/): A combined physical and genetic map of tandem repeat markers.

4. METHODS

4.1. Genotyping

Genotyping was performed to identify the X-linked gene locus in FDH, to investigate linkage to MHAC in Slovak family, and to fine-map the candidate gene loci in HBT. An initial genome scan on the HBT family members participating in the study had previously been performed as a service grant at the National Heart, Lung and Blood Institute (NHLBI) Mammalian Genotyping Service (Contract Number HV48141) using Marshfield Screening Set 16 that contained 402 microsatellite markers spanning autosomes and sex chromosomes with an average density of 10 cM (Weber and Broman, 2001). Error rate for genotyping was estimated as 0.5 per cent. Results were submitted to us in LINKAGE format. For FDH and MHAC families, genome scan was not necessary, as chromosome and genomic region of interest had been known, which were X-chromosome and 16p13.13-p12.2, respectively.

Markers for genotyping were selected from NCBI UniSTS database. Selection was based on reported locus heterogeneity and STR unit length. Primer sequences and amplification conditions were as reported in NCBI GenBank. The lists of the markers used in each of the fine mapping studies are given in Tables 4.1 and 4.2. One STR region, a $(TATC)_{12}$ repeat, was selected due to a lack of a suitable reported marker at the desired position. Named as C1615M, it was amplified using a pair of primers designed in this study. Primer sequences for this 227-bp amplicon were F: 5'CCATGCTTTTAGATACATACATTTG3' and R: 5'GCTGGTCCAACTCCTGTCTC3' and amplification was carried out in buffer A at the annealing temperature of 55°C.

Table 4.1. Chromosome 16 markers used to investigate linkage to MHAC and HBT loci and their physical and genetic positions. Eight markers used for fine-mapping HBT locus are indicated with asterisks.

Marker	Physical Position (bp)	Genetic Position (cM)	Marker	Physical Position (bp)	Genetic Position (cM)
D16S418	7579843	14.77	C1615M*	15884011	28.78
D16S768*	8311610	15.65	D16S764*	16554312	29.97
D16S678*	9199897	16.80	D16S490*	19383716	38.40
D16S497	10988018	22.16	D16S535*	19836721	38.51
D16S2640*	11335274	22.34	D16S403	22945152	43.87
D16S748	12046946	23.00	D16S672	24236302	43.89
D16S2619*	13650008	28.30	D16S690	27866135	57.79

Table 4.2. Markers used for X-chromosome scan in FDH and their physical and genetic positions. The twelve markers used for the initial scan are indicated with asterisks.

Marker	Physical Position (bp)	Genetic Position (cM)	Marker	Physical Position (bp)	Genetic Position (cM)
DXS6807*	4753382	13.50	DXS8107*	69637956	55.75
DXS9895*	7387107	15.66	DXS1124	71460705	56.76
DXS9902*	15233537	22.18	DXS8070	72572723	57.37
DXS6795*	23154421	29.76	DXS8060	73380734	57.37
DXS9896	29247081	30.84	DXS8092	74039691	57.37
DXS6810	42803634	42.75	DXS441	75273087	57.37
DXS8080*	44128374	44.85	DXS7131	76602179	57.37
DXS2501	44384144	46.54	DXS6800*	78567066	57.38
DXS8083	45126382	46.55	DXS8076	82666093	57.91
DXS1367	47574049	48.74	DXS8114	85500647	57.91
DXS1039	49345299	50.33	DXS6786	90313127	60.17
DXS8023	50370044	51.78	DXS6789	95336070	62.52
DXS2505	51837866	52.25	DXS6799	97265570	64.41
DXS2507	52627670	52.50	DXS454	97872777	64.71
DXS8017	53048169	52.50	DXS8020	99455381	65.50
DXS8062	53095822	52.50	DXS8063*	101084996	66.58
DXS1199	53739179	52.50	G10699	120705649	77.15
DXS1204	54126428	52.50	DXS1047*	128903001	82.07
DXS8032	54844449	52.51	D3S2390	140061921	87.56
DXS991	55535861	52.51	DXS8091*	147410548	96.14
DXS7132	64572061	52.51	DXS8087*	152547564	102.35
DXS6785	64679426	52.51	DXS1073*	153482102	102.35
DXS1213	65179522	52.51			

PCR amplifications were performed in 25 µl volumes of 1X reaction buffer, 0.4 µM of each primer, 0.2 mM of each dNTP, 20 ng of template DNA and 0.2 U of *Taq* DNA polymerase. The amplification program was as follows: initial denaturation (3 min at 94°C), 35 cycles of denaturation (30 sec at 94°C), annealing (30 sec at 50-60°C) and elongation (30 sec at 72°C) followed by a final extension (10 min at 72°C). In order to reduce slippage events and the resulting shadow bands during amplification of dinucleotide repeats, 1 X CES was added to the reaction. Amplification products were resolved by denaturing PAGE and visualized following silver nitrate staining to identify alleles. Exemplary gel pictures are given in Figure 4.1.

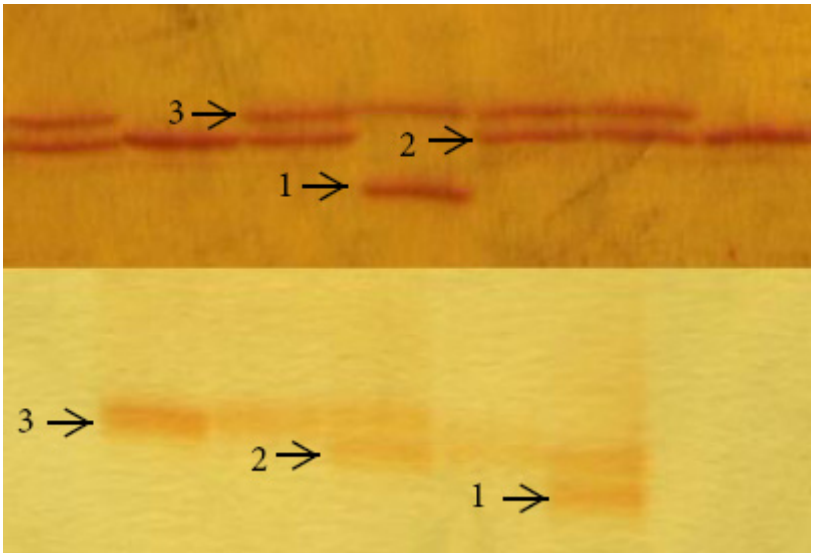

Figure 4.1. Examples of marker alleles resolved by denaturing PAGE. Bands on the upper gel are alleles of tetranucleotide repeat DXS2507, and bands on the lower gel of dinucleotide repeat D16S535. Alleles are numbered by ascending fragment size.

4.1.1. Denaturing Polyacrylamide Gel Electrophoresis

Alleles of microsatellite markers were resolved on a Sequi-Gen GT (BioRad, USA) gel electrophoresis system. Gels of 0.4 mm thickness were cast on either narrow (21 x 40 cm) or wide (38 x 30 cm) glass plates. Gel was prepared by the initiation of crosslinking in denaturing instagel solution with 10 per cent APS (8 µl per ml instagel) and TEMED (0.5 µl per ml instagel). It was allowed to set for at least 30 min. Gel was initially heated to 50°C by running with no loaded samples. Samples were mixed with equal volumes of 10 X loading buffer, denatured at 94°C for 5 min and kept on ice until loaded to wells on the gel formed

by a shark-tooth comb. The gel was run at constant power (35 W for narrow gels and 65 W for wide gels) for duration appropriate to the amplicon's size and microsatellite repeat unit length, for example 1 hour per 100 bp for dinucleotide repeat markers.

4.1.2. Silver Nitrate Staining

The gel was let cool down before gently separating the glass plates. It was transferred from the plate into staining buffer using a piece of wet filter paper. After 10 min, the gel was transferred to developing buffer and soaked for about 10 min until bands became visible. Whenever necessary, the process was repeated to enhance band visibility, intensively washing in-between.

4.1.3. Statistical Analyses

Reformatting of raw data for HBT family obtained from the genotyping service was necessary for analyses to be performed on easyLINKAGE platform, which allows the use of multiple linkage programs. This was accomplished by producing a Microsoft Excel Macro on Visual Basic for Applications. Marker maps were prepared by obtaining marker positions from NCBI UniSTS database and Rutgers second generation combined linkage and physical map of the human genome. Calculations were performed on easyLinkage platform (version 5.08) using PedCheck for detection of genotyping errors, SuperLink v1.6 for two-point parametric lod scores, Genehunter v2.1 for multipoint parametric lod scores and haplotypes building in small (bit size < 19) families and SimWalk v2.91 for multipoint parametric lod scores and haplotypes building in complex (bit size ≥ 19) families. Candidate loci deduced by computer analyses were fine mapped by genotyping with additional markers located around the loci. Fine mapping was performed also for FDH and MHAC families. Genotyping information obtained by fine mapping was then used in computer analyses.

4.2. Candidate Gene Approach

A disease gene locus is identified whenever statistical analysis yields lod scores > 3. Databases are then searched for candidate genes residing at this locus, with regard to expression profiles and functions possibly associated with the disease phenotype. The candidate gene's exons, splice junctions and regulatory sites are screened for sequence variation by SSCP analysis and/or DNA sequence analysis.

4.2.1. Analysis of Candidate Genes

Primer pairs for candidate gene exons and their flanking sequences were designed using software Primer 3. The sequences designed to analyze the candidate genes are given in Tables 4.3 to 4.6. Primer specificity was checked by *in silico* PCR. PCR amplification was carried out in a volume of 25 µl, containing 1X reaction buffer, 0.4 µM of each primer, 0.2 mM of each dNTP, 20 ng of template DNA and 0.2 U of *Taq* DNA polymerase. PCR program was as follows: Initial denaturation (3 min at 94°C), 35 cycles of denaturation (30 sec at 94°C), annealing (30 sec at appropriate temperature) and elongation (30 sec at 72°C) followed by a final extension (10 min at 72°C). Touchdown PCRs included an additional 10 cycles after initial denaturation, where annealing temperature was decreased 1°C per cycle from an initial 65°C. PCR products were checked for amplification by agarose gel electrophoresis: 5 µl of PCR product, mixed with 1 µl 6 X loading buffer, was loaded on a 2 per cent agarose gel containing 15 µg EtBr. The gel was run for 10-15 min for 150 volts in 0.5 X TBE buffer. The bands were subsequently visualized over a UV light transilluminator. PCR specificity was assessed by resolving the PCR products on denaturing PAGE.

Table 4.3. Sequences of primers, product sizes and reaction conditions for amplification and sequencing of *PORCN* as a candidate gene for FDH

Exon	Primer Sequence (5'>3')	Size (bp)	Buffer	Annealing Temperature (°C)
PORCN Exon 1	CTCAATCCTCCTGCTCCC CCTAGCACTCGCGCTACAG	318	Buffer A + CES	TouchDown to 56
PORCN Exon 2	CTGTGTCCCTGCTTTGACAG AATGTGGGAGGTCTGATATGG	250	Buffer A + CES	56
PORCN Exon 2'	CAGCCCCAAACTGAAATGTG TGGCTCGATATGGATGAATG	339	Buffer A + CES	TouchDown to 59
PORCN Exon 3	TCTCTTTCTCTCTCTTTCTCGTTC CCATGCACTTCAGCCAAC	298	Buffer A + CES	56
PORCN Exon 4	CTCAGAGGCCATGAGTGTCA CAGGTGAGGGAGAAAAGCAG	200	Buffer A + CES	56
PORCN Exon 5	CATGCTGATCTGCTCTCTGC AGGGTGGCTCCCACAGTC	280	Buffer A + CES	56
PORCN Exon 6	ACTGGTGAGGTCCTGAGTGG AGGCTCAGAACTGGGGAAAC	294	Buffer A + CES	56
PORCN Exon 7	AAGTGAGCACAGCCTTCGAG GACGGTCAGACACACTTGGA	237	Buffer A + CES	TouchDown to 58
PORCN Exon 8	ACTAACTGCCTGAGGGTGGA CAGGTCCCAACATGATACCC	239	Buffer A + CES	TouchDown to 58
PORCN Exon 9	GGGTATCATGTTGGGACCTG CCTCTAGGCAGCACCCTGT	230	Buffer A + CES	56
PORCN Exon 10	AACGGCCAAGACAGAAGTGT ATGAAAGGGCCTGGATTACC	228	Buffer A + CES	56
PORCN Exon 11	TGGGGGACTTTCAGGAGAAT GGGAATGCAGATGACAATGA	215	Buffer B	56
PORCN Exon 12	AGCAGGATCAGGGTGGAAG GGTAAGGGGGTCAGGTTAGC	237	Buffer A + CES	59
PORCN Exon 13	AGCCTCCCCTGAGGCTAAC CAGGCACCAAAAGAAGAAGG	247	N/A	N/A
PORCN Exon 13'	TACATGTGAGCAGGGTGGAG GATGCCAGCGAATAGAGGAG	506	Buffer B	54
PORCN Exon 14	GGGACACAGTGAGTAGGTCCA CAGCCTTTGTCCTCATGGTT	241	Buffer A + CES	TouchDown to 58
PORCN Exon 15	GCAAAGGATGGGTTTTCCTA CATCAGTGGCACCCTGAGA	231	Buffer A + CES	TouchDown to 58
PORCN 5' CpG	GTGCGCGGGTGACTATTT GCATACATTTCAGGCCCATA	848	Buffer A + CES	55
PORCN 3' UTR	TGTCCACAAGTGGTCAGAGC GGTTTCCAGCTTCCAAACCT	500	Buffer A + CES	TouchDown to 55

Table 4.4. Sequences of primers, product sizes and reaction conditions for amplification and sequencing of *C16ORF63* as a candidate gene for MHAC. Buffer of choice for these reactions was buffer A with CES.

Exon	Primer Sequence (5'>3')	Size (bp)	Annealing Temperature (°C)
C16ORF63 Exon 1	TATTGGCTACAGACCACGCC CCCTCACACCGAAGAATGAC	243	TouchDown to 58
C16ORF63 Exon 2	AAACATGGCTGGTGGTAGTG TTTTTGTGTCCCAGTCACCC	495	TouchDown to 59
C16ORF63 Exon 3	TTTTCCAACCAAACACTGGG TTATTCACTGCTGCACACCC	479	TouchDown to 59
C16ORF63 Exon 4	ATTTTGGATAATCATGCCGC ACCCTTCCCTGTCCAAGATT	476	TouchDown to 59
C16ORF63 Exon 5a	ACGCTTGGCCTCTGATTTC AAAAGATACCCCAAACAAAGCA	283	TouchDown to 58
C16ORF63 Exon 5b	GTGCATTTCAGATGACCACC CAGCTACTTGGGAGGCTGAG	436	63
C16ORF63 Exon 5c	AGTCTCGCTCTGTCACCCAG TCTGGCTCATCTGTGATTGC	595	TouchDown to 59
C16ORF63 Exon 5d	GGGATTTTTCAAAGATGGCA AATTTTACCAGCAGGGCCTC	577	TouchDown to 59

Table 4.5. Sequences of primers, product sizes and reaction conditions for amplification and sequencing of *PLK1* as a candidate gene for MHAC. Buffer of choice for these reactions was buffer B.

Exon	Primer Sequence (5'>3')	Size (bp)	Annealing Temperature (°C)
PLK1 Exon 1	CCGTGTCAATCAGGTTTTCC CTAGCAGCTCCAAGTCCCAG	749	TouchDown to 54
PLK1 Exon 2	GAGTCCAGTCCTGTGCTTCC AAAATATTGCATTGGGGCAC	414	TouchDown to 54
PLK1 Exon 3	GGGGTGAGAAGTGTCACTGG TTAGGCTTTGTTTGGGGATG	495	TouchDown to 54
PLK1 Exon 4	GGCCCTTAAGAATCCTGGTC TTTCAGACACAGGCCCTCTC	463	TouchDown to 54
PLK1 Exon 5	AAAGTGAGTTGGTGTTCGGC AACCACGGATTGAAGGACAG	581	TouchDown to 54
PLK1 Exon 6	GGAAGAGTTTCAGCTGTGGC ATGGTCCTATGCAGACAGGG	344	54
PLK1 Exon 7	ATGGGTCAGTGGAATGAAGG GATGGAGAGAGGAGGGCAC	461	TouchDown to 54
PLK1 Exons 8+9	TCAAACTCCTGGGCTCAAAC ATCCCAGAGGCCAGTGTATG	729	TouchDown to 54
PLK1 Exon 10	CATGTGGGTTGAATGTGGAG GCCTGGGGCTGATGAAG	699	TouchDown to 54

Table 4.6. Sequences of primers, product sizes and reaction conditions for amplification and sequencing of *NDE1* as a candidate gene for MHAC

Exon	Primer Sequence (5'>3')	Size (bp)	Buffer	Annealing Temperature (°C)
NDE1 Exon 1	AAAGTTTCCAAACGACGCTG	534	Buffer A + CES	TouchDown to 58
	AAGTCCCGGAAGGAGAAGAG			
NDE1 Exon 2	TTTTCTGTTAAAGGGGATCAGC	479	Buffer B	TouchDown to 54
	GGAGGCAGAGGTGCATCA			
NDE1 Exon 2'	GTAATTTCCATTCCAGCCCC	1122	Buffer A + CES	TouchDown to 58
	AGGCCTGCAATAAATGGTTG			
NDE1 Exon 3	TCCTTGAATTTGGCCAGGTA	576	Buffer B	TouchDown to 54
	CATTGCAGGGTTCCTTCTTC			
NDE1 Exon 4	TGAGACTCGGCCTCAAAAG	514	Buffer B	60
	AAATCCAGAAGGGCACTGG			
NDE1 Exon 5	TGGCATCTAGGAAGTTTGGG	318	Buffer B	54
	CTCAGGTAGGGAGAGGGGAC			
NDE1 Exon 6	CCTACTACCATGCTGGGCTA	475	Buffer B	TouchDown to 54
	GCTCTGAGCCTGATGCAAAT			
NDE1 Exon 7	TGTGATGCGGTTAACTACGG	299	Buffer B	TouchDown to 54
	CTGAAAGACAGGCAGGAAGG			
NDE1 Exon 8	CTGTCTGGGGTTCGTTCTTC	407	Buffer B	54
	AGACACCACCTAATGCTGCC			
NDE1 Exon 9	AGCGTTAATGCTCCATGGTC	373	Buffer B	TouchDown to 54
	AAGCTCTGGAAGAGGGGAAG			

4.2.2. SSCP Analysis

PORCN coding sequences in FDH patients and *C16ORF63* exons in Turkish MHAC patients were screened by SSCP for sequence variations. Exons 2 to 15 of *PORCN*, except exon 13, and all the exons of *C16ORF63* were analyzed with SSCP. *PORCN* Exon 13 could not be analyzed by this method as PCR optimization attempts failed. A second pair of primers were ordered and directly used for DNA sequencing analysis, since all the other exons had already been analyzed by SSCP and were at the process of sequencing at that stage.

For SSCP analysis, denatured PCR amplification products of control and patient DNA were electrophoresed on non-denaturing polyacrylamide gels. Gels were cast between glass plates 20 cm x 20 cm, assembled using 0.75 mm spacers. Gel solution was prepared from 40 per cent acrylamide stock with final concentrations of 8 per cent acrylamide-bisacrylamide, 0.6 X TBE in 30 ml. Two gels were prepared and run for each

analysis, one of them containing 5 per cent glycerol. Gel polymerization was initiated by adding 300 µl 10 per cent APS and 30 µl TEMED and vortexing. Fifteen-well combs were inserted after pouring the gel solution between the plates. Electrophoresis was carried out in 0.6 X TBE and 4°C. The gels were loaded with 10 µl of PCR products, which have been mixed with equal volume of 10X loading buffer and denatured at 94°C for 5 min. The gels were run in BioRad DCode Universal Mutation Detection System. Electrophoresis conditions were constant power of 10 W for 8-16 hours depending on product length. Gels were stained with silver nitrate after electrophoresis.

SSCP analysis has low resolution and may yield false-negative results; thus, DNA sequencing analysis was subsequently performed to confirm the SSCP results.

4.2.3. DNA Sequencing

PCR amplification products were purified with QIAquick PCR Purification Kit and sent together with sequencing primers to either of the two commercial firms, Iontek (Istanbul, Turkey) or RefGen (Ankara, Turkey), where DNA sequence was generated by automated dye-terminator sequencing. Results were obtained in the form of chromatograms and compared to NCBI and USCS databases by eye and also by using sequence analysis programs.

All candidate gene exons plus the assumed promoter of *PORCN* were sequence analyzed. Tables giving the coverage of flanking sequences of analyzed loci are listed in results section.

Exon 2 of *NDE1* was refractory to PCR amplification. Deletion of the exon was hypothesized, and primers specific to various sites in introns 1 and 2 were designed to identify the deletion breakpoints by normal and long PCR reactions (Table 4.7).

Table 4.7. Sequences of primers, product sizes and reaction conditions for amplification and sequencing of exon 2 of *NDE1* in MHAC patients

Exon	Primer Sequence (5'>3')	Size (bp)	Buffer	Annealing Temperature (°C)
NDE1 Del #1	ACCCATTTTGAGCCTTTCCT CTTGTGAAGAGCCAGTGCAA	14944	Long PCR Kit	55
NDE1 Del #2	GGCATACGGTGTTTCTGCTT CTTGTGAAGAGCCAGTGCAA	11908	Long PCR Kit	55
NDE1 Del #3	TGTGGCTGGGACATAAGTGA CTTGTGAAGAGCCAGTGCAA	9812	Long PCR Kit	55
NDE1 Del #4	AGGGATACACACCAGCCTCT CTTGTGAAGAGCCAGTGCAA	7320	Long PCR Kit	55
NDE1 Del #5	CCTTAACCCACCCACCTACC CTTGTGAAGAGCCAGTGCAA	5565	Long PCR Kit (Buffer A + CES)	55 (58)
NDE1 Del #6	AAGCAGGAGAGCCCATCATA CTTGTGAAGAGCCAGTGCAA	3713	Long PCR Kit	55
NDE1 Del #6'	AAGCAGGAGAGCCCATCATA CATTGCAGGGTTCCTTCTTC	4555	Long PCR Kit	55
NDE1 Del #7	CCTTAACCCACCCACCTACC TCACCTGAGGTTGGGAGTTC	4874	Buffer A + CES	58
NDE1 Del #8	TGAGTCTCGCTCTGTCACCC ATGGTGGCTCATGCCTGTA	N/A	N/A	N/A

4.2.4. Determination of Relative *PORCN* Transcript Levels

Ten ml of fresh blood samples obtained from affected individuals 302 and 304 in FDH family were treated with 3 volumes of cell lysis buffer for 15 min at 4°C to lyse red blood cells. The pellet obtained by centrifugation at 5000 revolutions per minute (rpm) and 4°C for 10 min, which consisted of white blood cells, was used to extract total RNA using RNeasy Mini Kit (Qiagen, USA). Reverse transcription of RNA samples was achieved by using Transcriptor First Strand cDNA Synthesis Kit (Roche, Germany). Real time quantitative PCR was performed on these cDNA samples, along with cDNAs from a healthy individual as calibrator, using primers designed for this purpose (Table 4.8). *HPRT1* was used as the control gene. Quantification PCRs were prepared with LightCycler 480 DNA SYBR Green I Master (Roche, Germany) and were run on a LightCycler 480 (Roche, Germany) in triplicates. Transcript levels were calculated using LightCycler 480 Relative Quantification Software (Roche, Germany).

Table 4.8. Primer sequences and product sizes for quantitative PCR assay of *PORCN* transcripts

Gene	Primer Sequence (5'>3')	cDNA size (bp)	gDNA size (bp)
PORCN	AACGGTGACCGCCTCCTT	53-86	1573
	GAGACAGCACTCTCGTAGGC		
HPRT1	TGACCTTGATTTATTTTGCATACC	102	1712
	CGAGCAAGACGTTCAGTCCT		

5. RESULTS

5. 1. FDH

Prior to this study several individuals in a large family had been diagnosed with focal dermal hypoplasia (Seven *et al.,* 1998). Inheritance pattern for this disease is dominant X-linked with *in utero* male lethality. On this basis, this study was initiated with the purpose of identifying first the disease gene locus and then the genetic defect that gives rise to the clinical manifestations.

5.1.1. Linkage Analysis

Peripheral blood samples had been obtained from fourteen members of the family (Figure 5.1) and genomic DNA extracted.

The approach used for linkage analysis in this study was genotyping the family with microsatellite markers in order to obtain haplotypes and calculate "logarithm of odds" (LOD) scores. Since the disease was hypothesized to be X-linked dominant, only markers specific to the X-chromosome were used. Initially the entire X-chromosome was scanned at approximately 15-cM intervals using 12 markers (Table 4.2). The genotypes obtained from informative markers were used to construct haplotypes. A haplotype fully segregating with the disease was observed, as well as positive LOD scores for the markers of the haplotype. The region covered by the haplotype was 23-101 Mb and was further analyzed with 30 markers (Table 4.2), finally narrowing down to 47.5-99.4 Mb, between markers DXS1367 and DXS8020 (Figure 5.1). In this interval the multipoint parametric LOD score peaked at 3.29 (Figure 5.2), which is above the value for accepting linkage (LOD > 3).

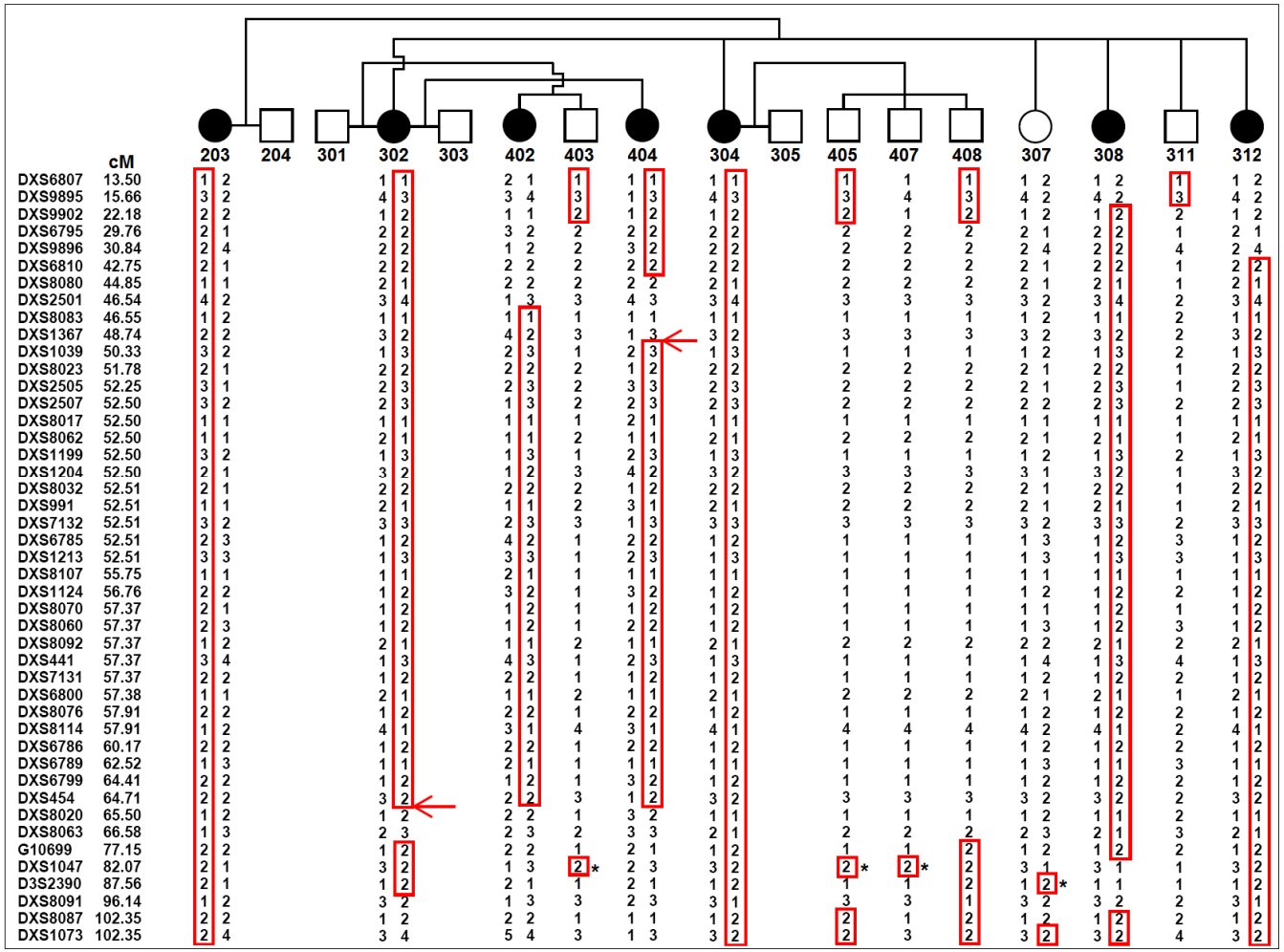

Figure 5.1. Haplotypes of FDH family at Xpter-qter. The haplotype harboring the disease locus is boxed, and the delimiting crossovers are shown with arrows. Possible mistypings identified by non-Mendelian error tests are indicated by asterisks.

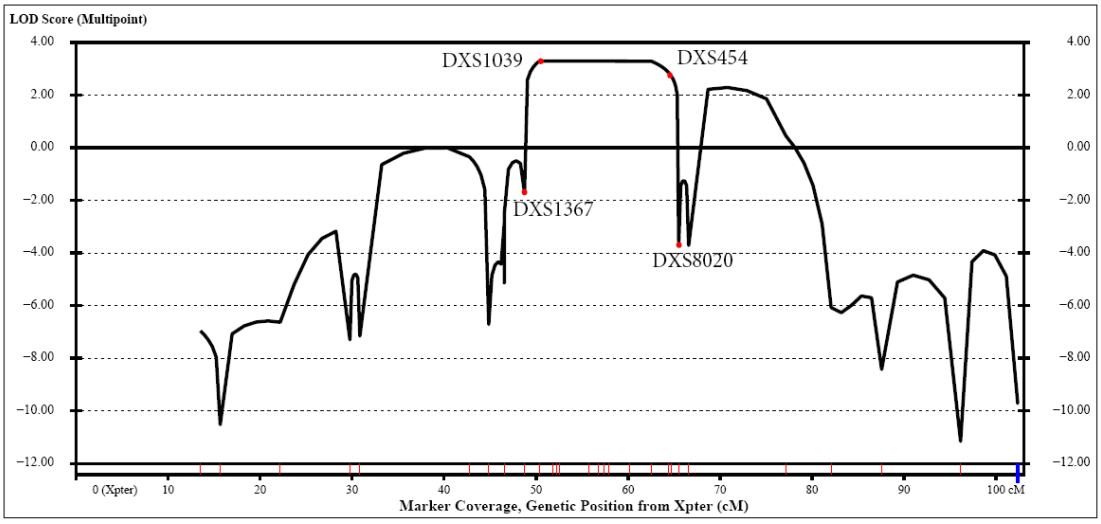

Figure 5.2. Multipoint linkage analysis at Xpter-qter. Markers defining the FDH locus are designated on the graph.

5.1.2. Analysis of *PORCN* Gene

Linkage analysis in FDH patients resulted in significant linkage to a ~52-Mb region, roughly one third of the X-chromosome. Fine mapping to narrow down the disease locus did not reveal any further crossovers. DNA samples from other members of the family were not available to use for further attempts to refine the disease locus. Of the 1529 genes localized to the chromosome, 489 resided at this locus. Application of candidate gene approach was not practical due to the sheer number of genes.

At this stage of the study, two reports were published that identified defects in *PORCN* as the underlying cause for FDH (Grzeschik *et al.,* 2007; Wang *et al.,* 2007). Therefore, this gene was analyzed for mutations in the family studied. Initially, all coding exons of *PORCN* were analyzed by SSCP (except exon 13, see section 4.3.2.). SSCP patterns for exon 12 were suspected to imply sequence variations (Figure 5.3). Those fragments were subjected to DNA sequence analysis, but no difference between control and patient DNA was observed. Then, the remaining coding exons were sequenced, again no difference was found. Therefore, some non-coding regions of *PORCN* gene were also analyzed, namely the 5' untranslated region (UTR) (including exon 1 and part of exon 2) and 3' UTR (within exon 15). Furthermore, a putative proximal promoter was suspected to exist in the CpG island lying within 1000 bases upstream of the transcription initiation site,

so this region was also sequenced. These analyses also resulted in no mutation detection. Sequence analysis coverage is listed in Table 5.1.

Table 5.1. Sequenced regions of *PORCN*

PORCN Target Region	Extent of Sequencing	
	5' of the Target Region	3' of the Target Region
PROMOTER (CpG island)	-80	+126
EXON 1	-93	+23
EXON 2	-73	+26
EXON 3	-34	+29
EXON 4	-30	+64
EXON 5	-31	+29
EXON 6	-65	+37
EXON 7	-73	+82
EXON 8	-115	+41
EXON 9	-37	+28
EXON 10	-34	+32
EXON 11	-46	+46
EXON 12	-64	+40
EXON 13	-220	+148
EXON 14	-31	+34
EXON 15	-26	+60

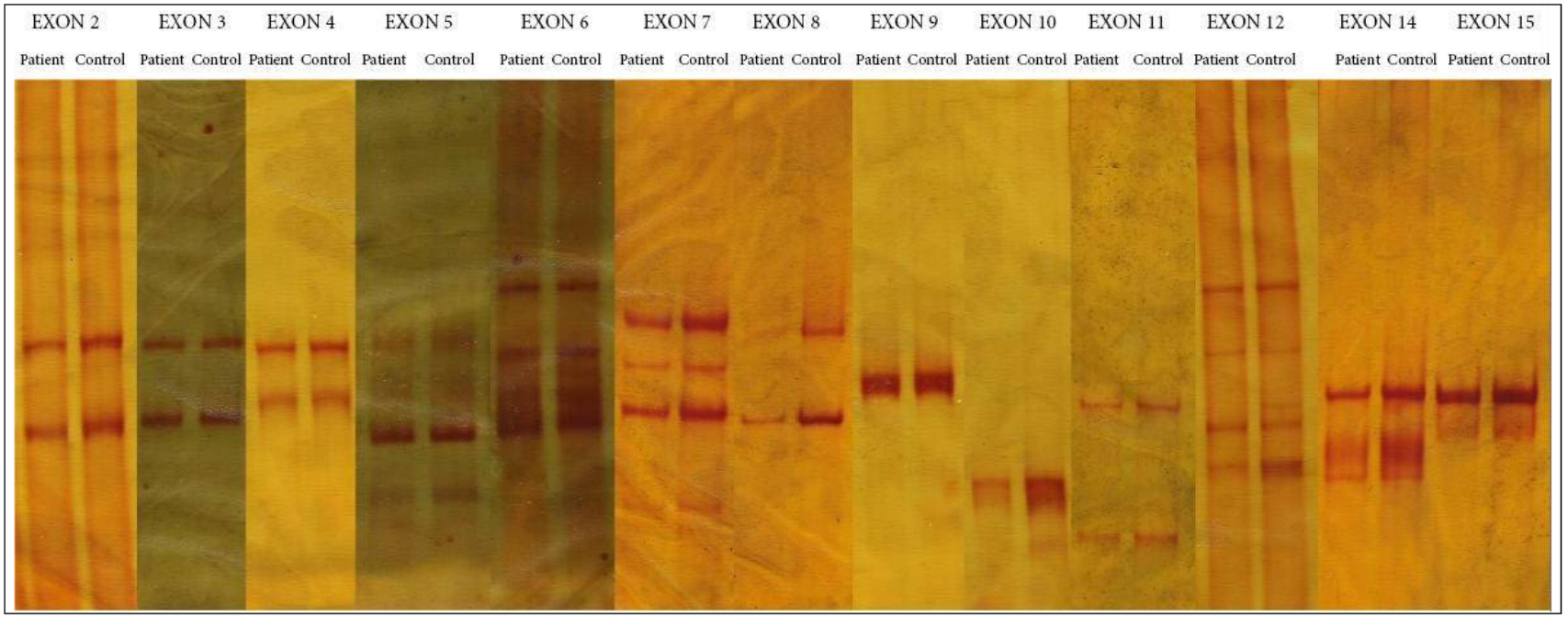

Figure 5.3. SSCP analysis of *PORCN* coding exons

Sequencing did not reveal any mutation in *PORCN* exons, untranslated regions and the putative promoter. A mutation in a regulatory region of *PORCN* is expected to cause aberrant gene expression. In order to assess whether gene expression had been affected, transcript levels of *PORCN* in two patients was investigated by real time qPCR. Primers amplifying an intron spanning region from exon 6 to exon 9 were designed. These primers are expected to amplify cDNA to yield four fragments with lengths of 86 bp (from isoform D), 71 bp (isoform C), 68 bp (isoform B), and 53 bp (isoform A and E). The 68-bp fragment from isoform B could not be amplified from either the reference RNA or patient RNAs. The fragments corresponding to different isoforms are presented in Figure 5.4

The results indicated that *PORCN* expression is reduced in comparison to the healthy control (Table 5.4). Relative transcript levels are 50 per cent decreased in patient 302 and 80 per cent in 304. The level of reduction is consistent with severity of symptoms, as individual 304 has a more severe phenotype than individual 302.

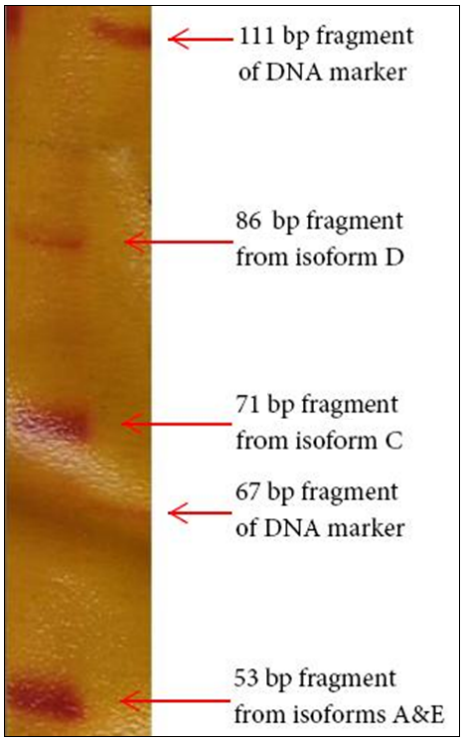

Figure 5.4. Amplification of intron spanning *PORCN* primers from reference RNA

Table 5.2. Transcript levels of *PORCN* in FDH patients relative to *HPRT1*

RNA Sample	Expression Ratios
Reference	1.000
302	0.48
304	0.20

5.2. MHAC

Autosomal recessive microhydranencephaly, an inherited condition of extreme rarity, was previously described in a large consanguineous Anatolian family by Kavaslar *et al.* (2000). The disease locus was mapped by linkage analysis to a region in the short arm of chromosome 16, defined by microsatellite markers D16S497 (10988018 bp) and D16S672 (24236302 bp).

5.2.1. Linkage Analysis

In a non-consanguineous Slovak family, two male siblings exhibited a clinical picture very similar to MHAC. Thus, the disease was suspected to have the same genetic etiology, and genotyping and subsequent linkage analysis was conducted to determine whether the disease locus was the same. If it was, narrowing down MHAC locus might have been possible, simplifying candidate gene approach.

Genomic DNA samples from peripheral blood cells were provided from the siblings and their parents by Dr. Jana Behunova. The samples were amplified with microsatellite markers surrounding MHAC locus to determine genotypes (Table 4.1). Haplotypes were constructed (Figure 5.5), and haplotype inspection revealed that the two siblings inherited alternate maternal chromosomes, indicating that this locus is not linked to the condition. This fact is further supported by multipoint LOD scores of the region, which are below the threshold for exclusion (LOD < -2) (Figure 5.6).

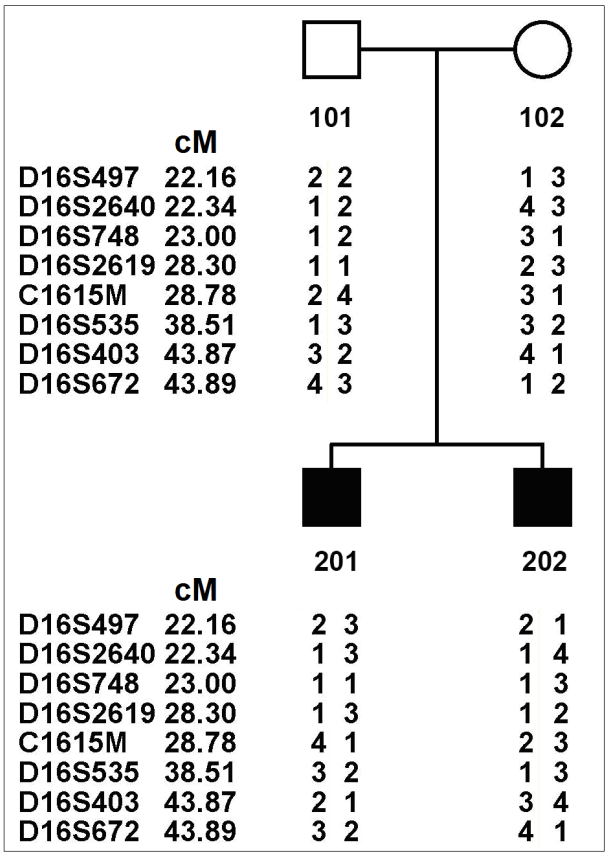

Figure 5.5. Haplotypes of Slovak family at 16p13.13-p12.1

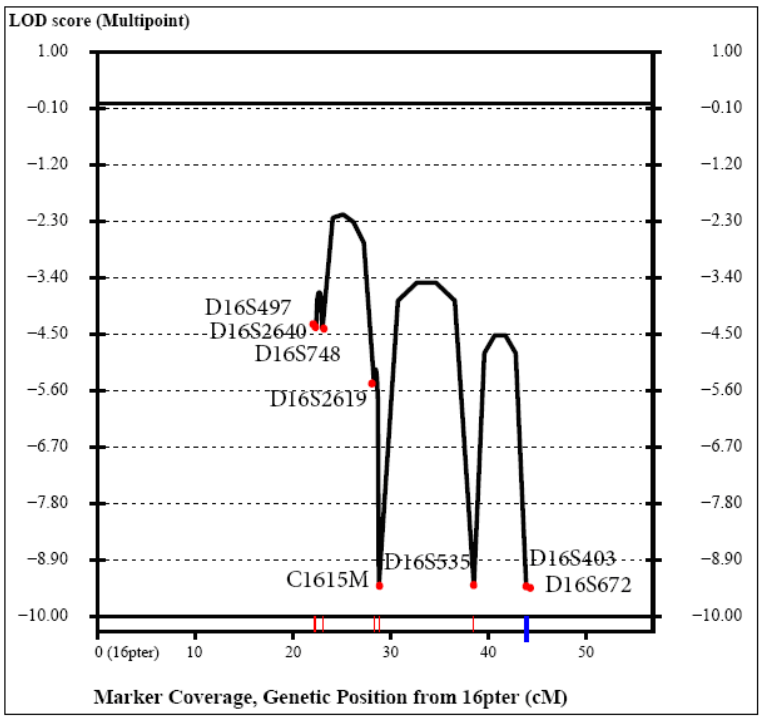

Figure 5.6. Multipoint linkage analysis at 16p13.13-p12.1. Microsatellite markers used in this study are designated on the graph.

While this study was in progress, mother of patients 1 and 3 in the subject family of Kavaslar *et al*. (2000) became pregnant. Because developmental abnormalities associated with MHAC do not become apparent until after the time limit for abortion, *in utero* methods can not be utilized for timely diagnosis of MHAC. Therefore, genotyping the fetus was necessary for genetic diagnosis. For this purpose, clinicians performed chorionic villus sampling and subsequent genomic DNA extraction. Upon receiving the DNA sample, it was analyzed along with samples from the parents and the affected siblings using six microsatellite markers that cover MHAC locus. Subsequent construction of haplotypes revealed that the fetus was only heterozygous for the disease haplotype (Figure 5.7).

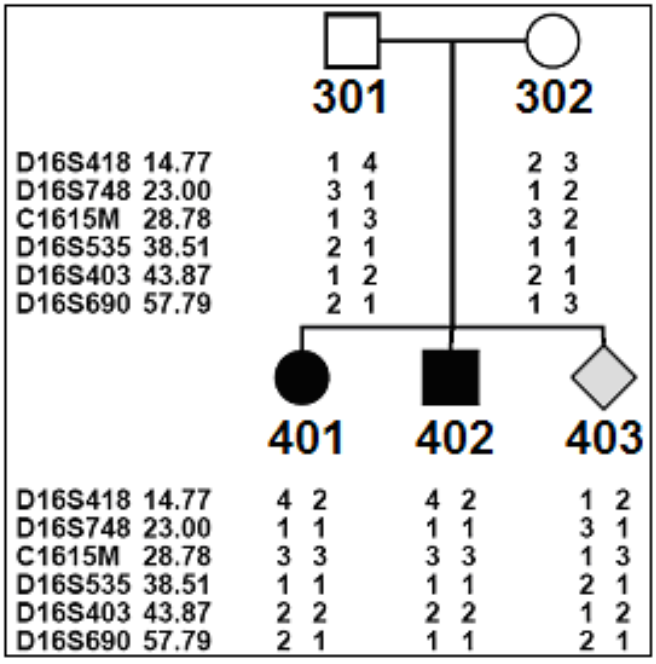

Figure 5.7. Haplotypes of the fetus, her parents and affected siblings in the Anatolian MHAC family at 16p13.2-p11.2

5.2.2. Candidate Gene Approach

As the genotyping for the Slovak family were ongoing, a research group in France discovered a novel gene at open reading frame (ORF) 63 on chromosome 16. The gene resides at the MHAC locus, and although the discovering group generally kept the function of the gene classified, they provided us with information sufficient to assess the gene as a candidate to be responsible for MHAC. Thus, the exons were analyzed for sequence

variations in patients. SSCP analysis results are compiled in Figures 5.8 and 5.9. Aberrant SSCP migration patterns were observed in exons 3, 5A and 5D. Regardless of SSCP analysis findings, all exons were sequenced. The extent of sequencing is presented in Table 5.3. Differences between the patient and reference sequences in 2 previously reported SNP sites were detected (Table 5.4). Besides these SNPs, no deviation from reference sequence was observed in patient DNA. In addition, the control DNA was heterozygous for a novel polymorphism in intron 4: c.311+102A>C (Figure 5.10). This polymorphism was not reported in NCBI SNP database.

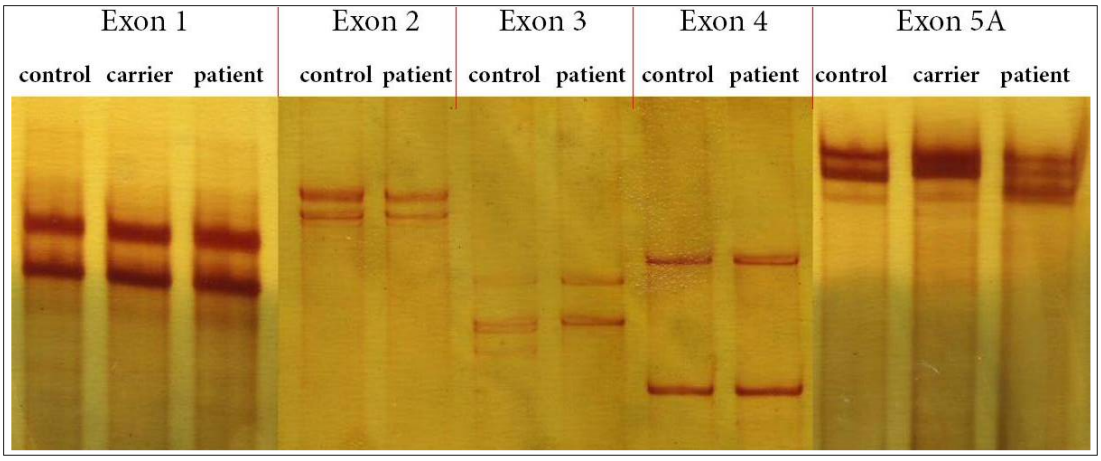

Figure 5.8. SSCP analysis of *C16ORF63* coding regions

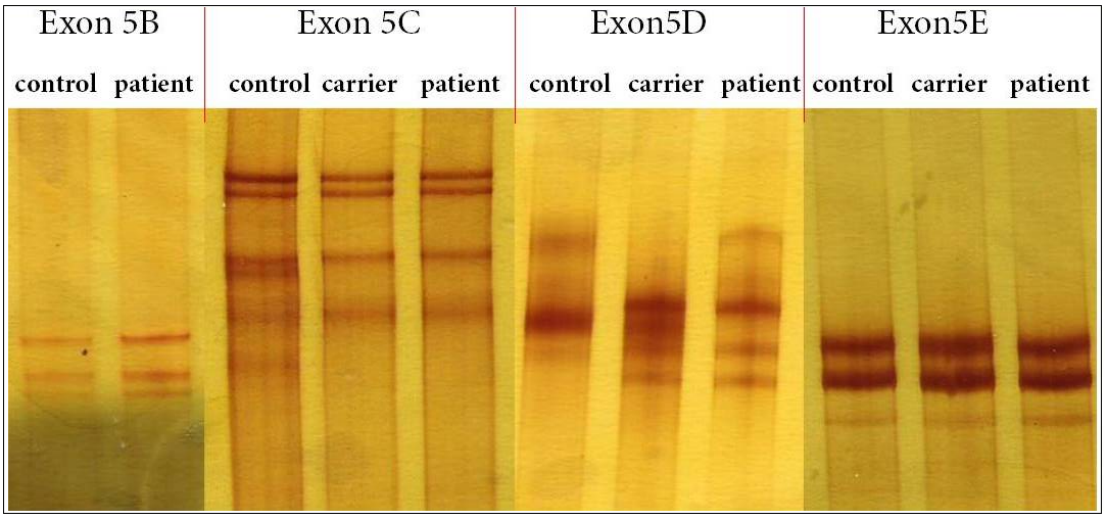

Figure 5.9. SSCP analysis of *C16ORF63* 5' UTR

Table 5.3. Sequenced regions of *C16ORF63*

C16ORF63 Target Region	Extent of Sequencing	
	5' of the Exon	3' of the Exon
EXON 1	-61	+80
EXON 2	-123	+105
EXON 3	-204	+128
EXON 4	-133	+122
EXON 5	-144	+31

Table 5.4. SNPs found in the patient in *C16ORF63* gene

Amplicon	SNP ID
C16ORF63 EXON3	rs12598817
C16ORF63 EXON5E	rs3833040

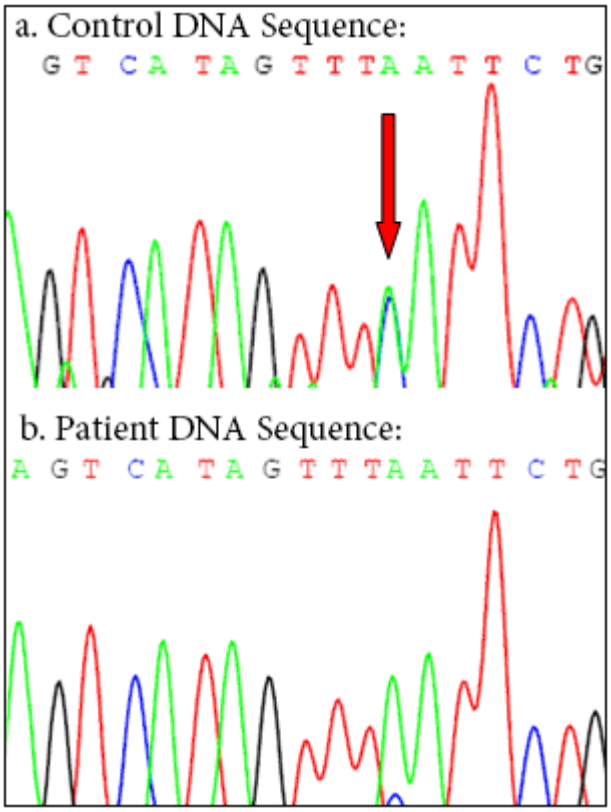

Figure 5.10. Novel SNP in intron 4 of *C16ORF63*. The A/C double peak is shown with an arrow.

As the analysis of *C16ORF63* exons was completed and results indicated no relation between MHAC and the gene, a report relating mitotic spindle defects to microcephaly was published (Rauch *et al.,* 2008). It reported that pericentrin gene mutations that disrupted spindle formation underlie microcephalic osteodysplastic primordial dwarfism type II. The report also drew attention to the fact that defects in similar spindle related genes were previously found in other primary microcephaly types (CDK5RAP2: MCPH3; ASPM: MCPH5; CENPJ: MCPH6). Accordingly, the 158 genes at MHAC locus were evaluated for possible functions in mitotic spindle formation. Two genes emerged as strong candidates: polo-like kinase 1 (*PLK1*) and nuclear distribution gene E homolog 1 (*NDE1*).

Exons of *NDE1* and *PLK1* were analyzed by DNA sequencing in patients. All conformed to reference sequence, with the exception of *NDE1* exon 2, which could not be amplified from patient DNA. The extent of sequence determined is given in Tables 5.5 and 5.6. No sequence variation was found.

Table 5.5. Sequenced regions of *PLK1*

PLK1 Target Region	Extent of Sequencing	
	5’ of the Exon	3’ of the Exon
EXON 1	-131	94
EXON 2	-70	103
EXON 3	-158	127
EXON 4	-181	121
EXON 5	-191	115
EXON 6	-50	73
EXON 7	-218	101
EXON 8&9	-87	134
EXON 10	-75	55

Table 5.6. Sequenced regions of *NDE1*

NDE1 Target Region	Extent of Sequencing	
	5' of the Exon	3' of the Exon
EXON 1	-68	284
EXON 3	-285	69
EXON 4	-210	90
EXON 5	-84	31
EXON 6	-142	85
EXON 7	-115	29
EXON 8	-80	116
EXON 9 (coding part)	-144	92

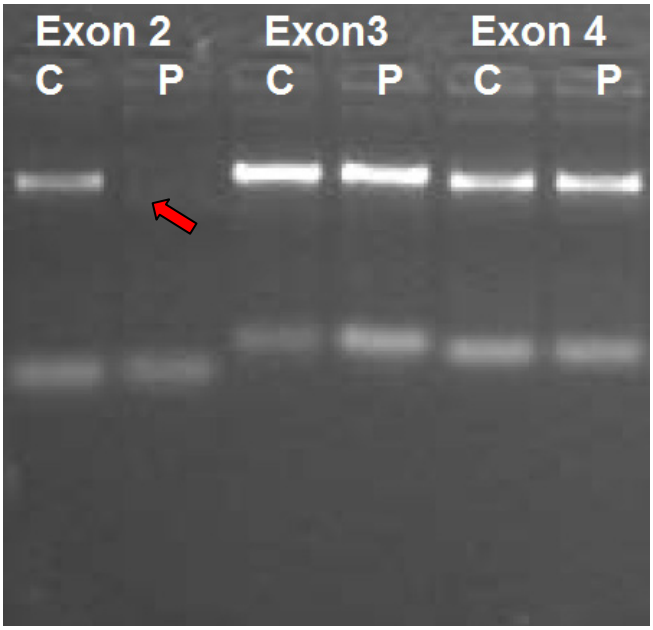

Figure 5.11. Agarose gel electrophoresis of PCR products of amplification of *NDE1* exons 2-4 in control (C) and patient (P). Arrow points to the absence of product.

Repeated failure to amplify *NDE1* exon 2 in MHAC patients (Figure 5.11) could be interpreted in two alternative ways: Either an SNP in a primer binding site prevented primer binding or a deletion abolished a primer binding site. The first alternative was tested by both lowering the annealing temperature in PCR reactions and designing a new set of primers flanking the exon (Table 4.6). Neither approach was fruitful. The second alternative was tested by applying long-PCR, using the forward primer of exon 1 and the reverse primer of exon 3. This amplicon, on reference sequence, contains exons 1, 2 and 3 along with introns 1 and 2, with a total length of 17422 base pairs. Such a long

amplification was normally beyond the reach of the long PCR kit, yet, with a sufficiently large deletion in the template DNA, it could be possible. PCR products were obtained from patient and carrier DNAs but not control DNAs (Figure 5.12). The product was about 12-14 kilo base pairs (kb) long, strongly suggesting the presence of a deletion estimated about 3-5 kb.

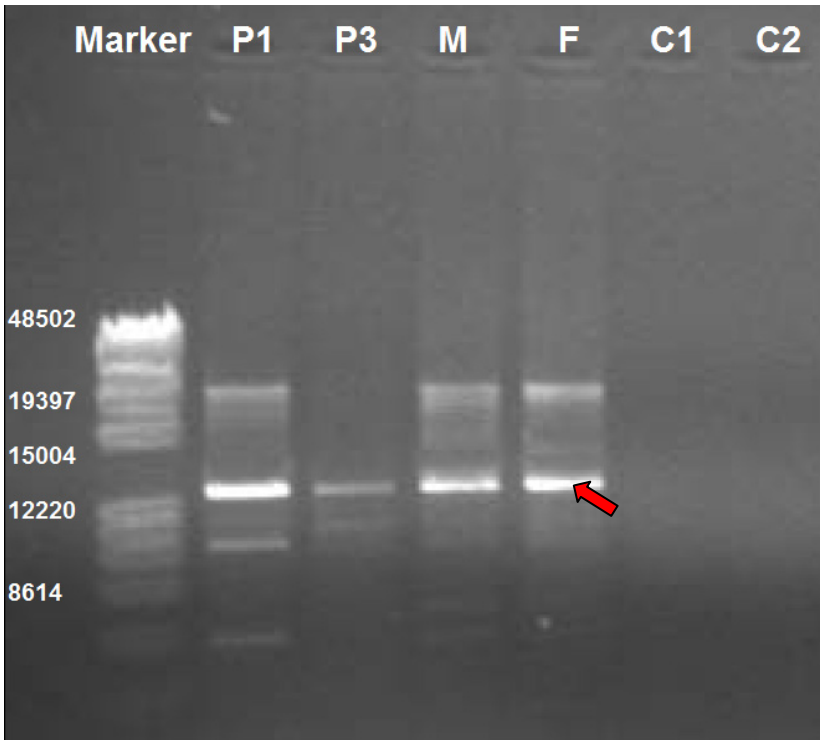

Figure 5.12. Agarose gel electrophoresis of long-PCR products. Amplification from exon 1 through exon 3 in affected siblings (P1, P3), their parents (M, F) and controls (C1, C2). Arrow points at amplification products that are shorter than reference sequence.

The length of the deletion was apparently more than 3400 bp, since the long-PCR product length was about 12-14 kb. Amplification using primers flanking a region consisting of exon 1, intron 1 and exon 2 failed. Considering the lengths of intron 1 (14441 bp), exon 2 (126 bp) and intron 2 (2424 bp), the deletion most likely started within intron 1 and ended in intron 2. To identify the deletion breakpoints, six forward and two reverse primers were designed at a few sites possibly closer to the deletion and used in various combinations for PCR (Table 4.7). The shortest amplicon was tested first, and only primer pair NDE1 Del #5 lead to a successful amplification in patients (Figure 5.13).

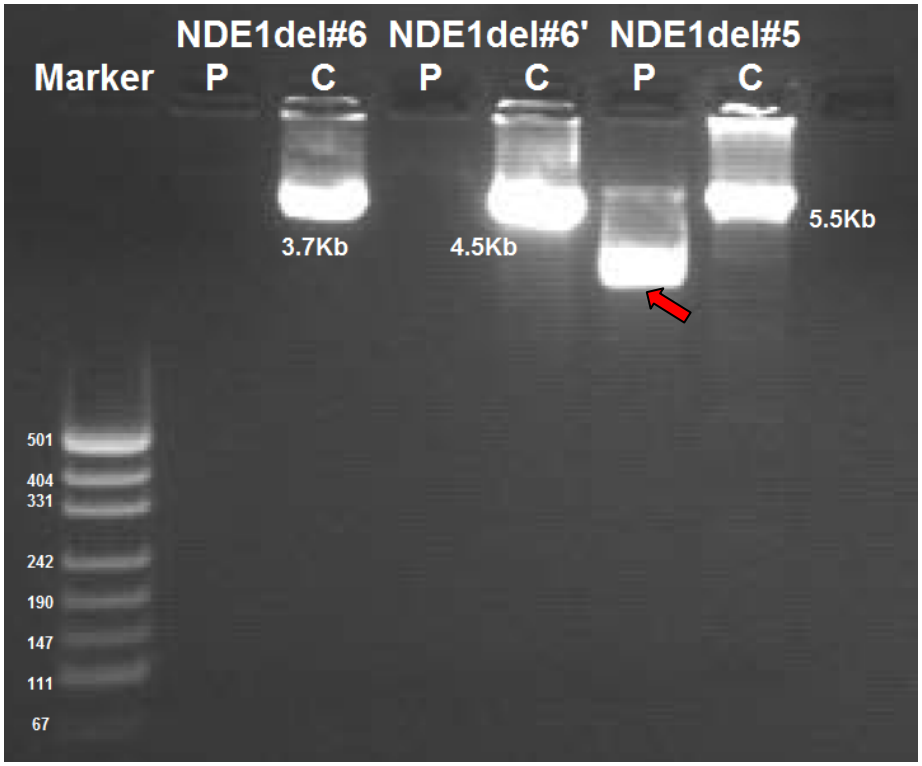

Figure 5.13. Agarose gel electrophoresis of PCR products of primers flanking *NDE1* exon 2. M: DNA marker, P: Patient DNA, C: Control DNA. Arrow points at the amplification product from patient DNA, which is shorter than reference sequence.

PCR product obtained by using primer pair NDE1 del#5 was sequenced in both directions. Forward sequencing was of very low quality, because the polydT-stretch downstream the primer binding site seemed to lead to replication slippage. Reverse sequencing fell short of the deletion breakpoint, and another reverse primer (NDE1 del#7-R) was designed to reach it (Figure 5.14). Subsequent sequencing with this primer was also interfered by a polydT-stretch before reaching the deletion. Using a third reverse primer (NDE1 del#8-R) immediately upstream of the polydT, however, clearly revealed the deletion breakpoint (Figure 5.15), which turned out to be 15 bp downstream of the polydT stretch that interfered with forward sequencing. The deletion, c.1-3548_83+644del, had removed 4275 bp, including exon 2 and the translational start site of the gene. The deletion obviously occurred due to an unequal crossover event between the two copies of a 56-bp directly repeated sequence, with 91 per cent homology.

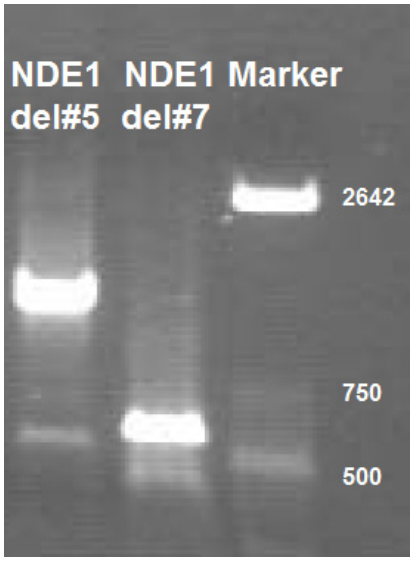

Figure 5.14. Agarose gel electrophoresis of PCR products of primers flanking *NDE1* exon 2 in patient 1

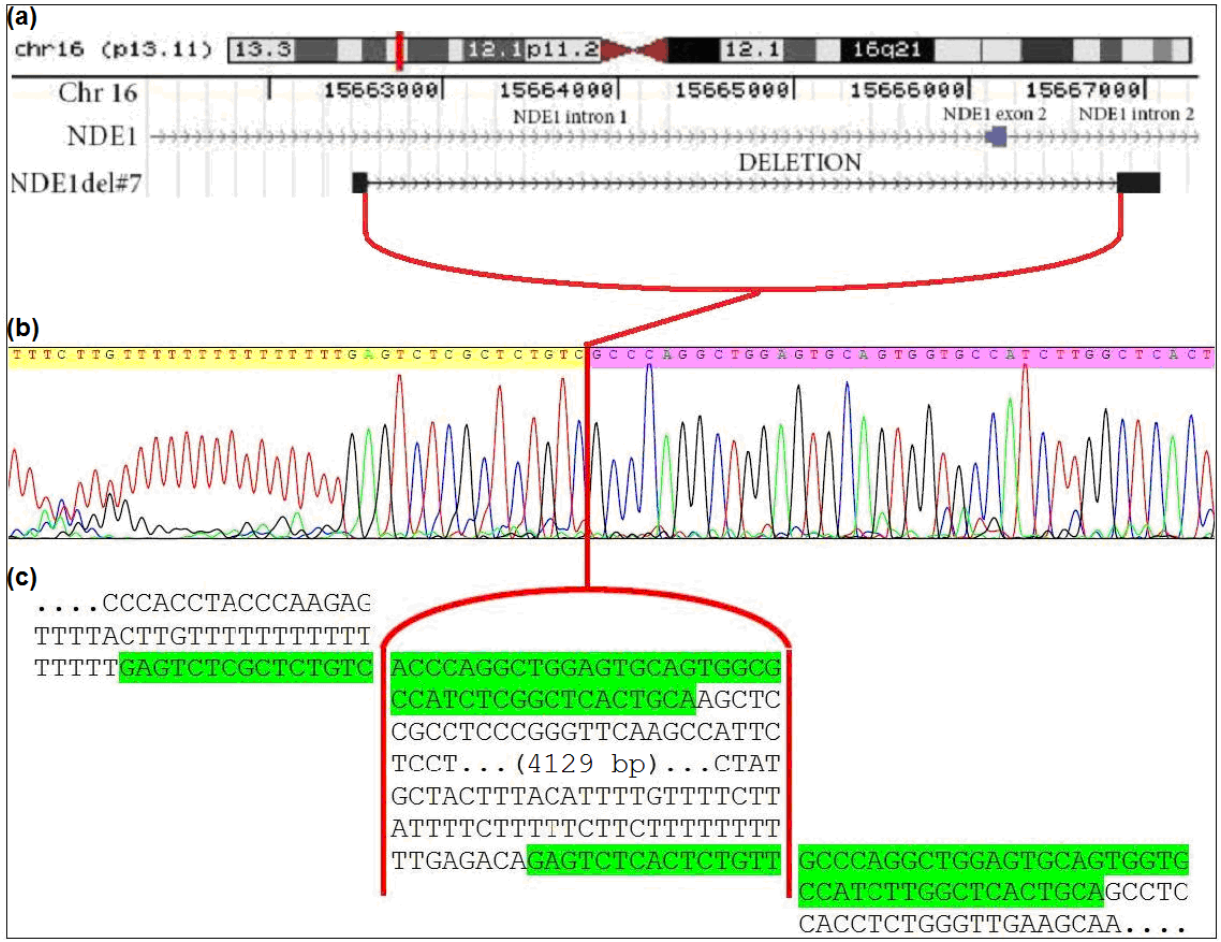

Figure 5.15. *NDE1* deletion breakpoints. (a) Alignment of the NDE1del#7 amplicon from MHAC patient to the reference sequence. (b) Chromatogram showing the sequences of deletion breakpoints. Slippage in the polydT region causes double peaks in the 5' region. (c) Flanking sequences of *NDE1* deletion breakpoints. Copies of the 56-bp repeat are highlighted in green.

5.3. Hereditary Brain Tumors

5.3.1. Linkage Analysis

In a family of five siblings and their sibs, two forms of brain tumors were observed in two generations. The tumors were either grade IV astrocytomas (glioblastoma multiforme) or meningiomas. The frequent occurrence of tumors in the family was attributed to a hereditary susceptibility to tumor formation. To test this hypothesis, linkage studies for the family were conducted. DNA samples of fifteen family members had been already subjected to genome scan. The genotyping results were used for calculating lod scores and constructing haplotypes. Lod score calculation parameters were dominant inheritance assuming either full (Figure 5.16) or 70 per cent penetrance (Figure 5.17). Unaffected parents 201 and 203 were assumed 'affected' for statistical analyses since they were obligate carriers, both having an affected child. Under full penetrance, the peak at chromosome 16p had a lod score of 3.01. When 70 per cent penetrance was assumed, the region lost significance (LOD=2.32) and other peaks with lower positive lod scores were also observed.

In an attempt to localize the disease gene, the region around the peak at chromosome 16p was fine-mapped. The family members were genotyped with eight additional markers, the resulting genotype data was used to calculate the multipoint LOD scores at full penetrance (Figure 5.18), and haplotypes were constructed (Figure 5.19). Both LOD scores and inspection of haplotypes confirmed that a ~5.3-Mb region between markers D16S768 and D16S2619 segregated with the condition. The minimum critical region for the locus was delineated by markers D16S678 and ATA3A07 (D16S748), spanning ~2.8 Mb.

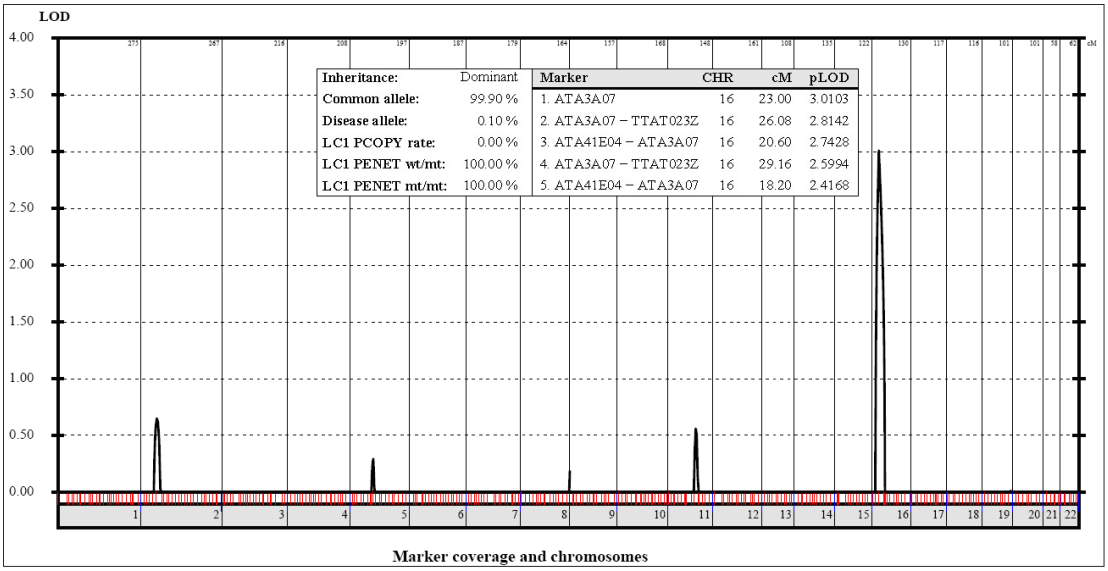

Figure 5.16. Multipoint LOD scores of the autosomal data set generated by the genome scan, in a dominant model with full penetrance. Lod scores are plotted in the order of chromosomal position. Top five scores are given within the graph.

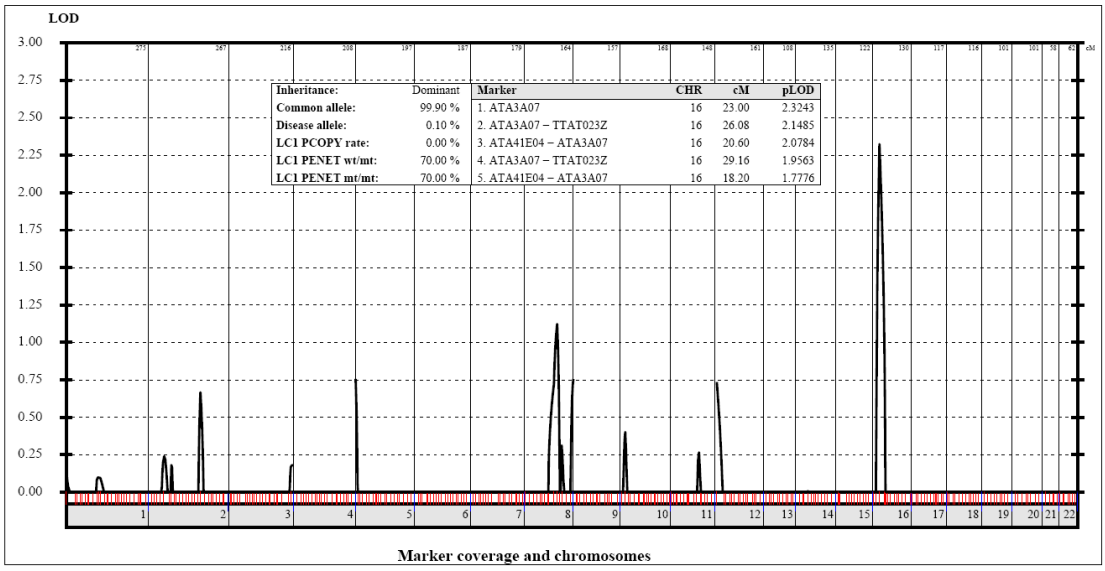

Figure 5.17. Multipoint LOD scores of the autosomal data set generated by the genome scan, in a dominant model with 70 per cent penetrance. Lod scores are plotted in the order of chromosomal position. Top five scores are given within the graph.

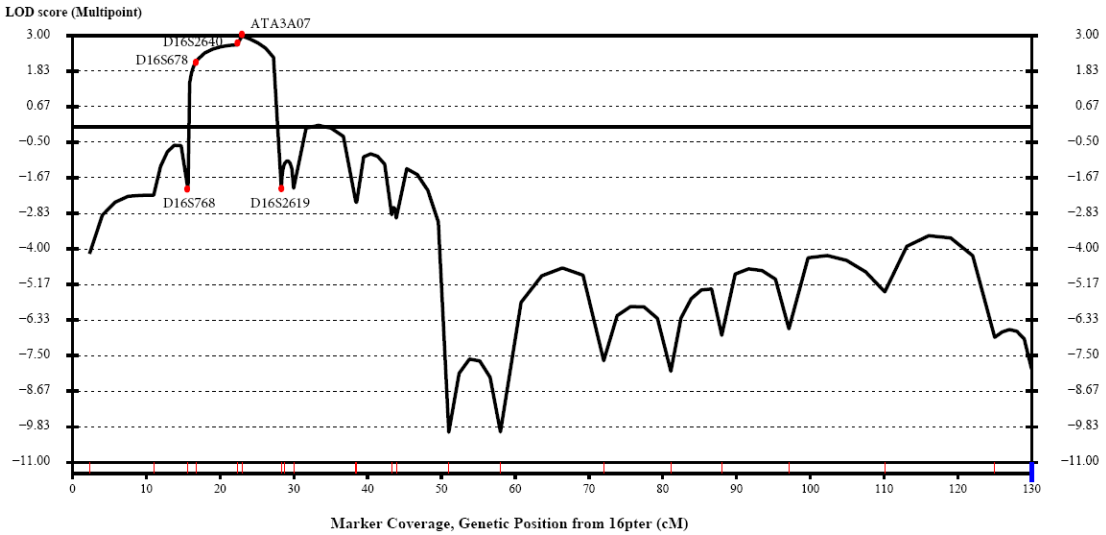

Figure 5.18. Multipoint linkage analysis at 16pter-qter assuming full penetrance. Markers defining the FDH locus are designated on the graph.

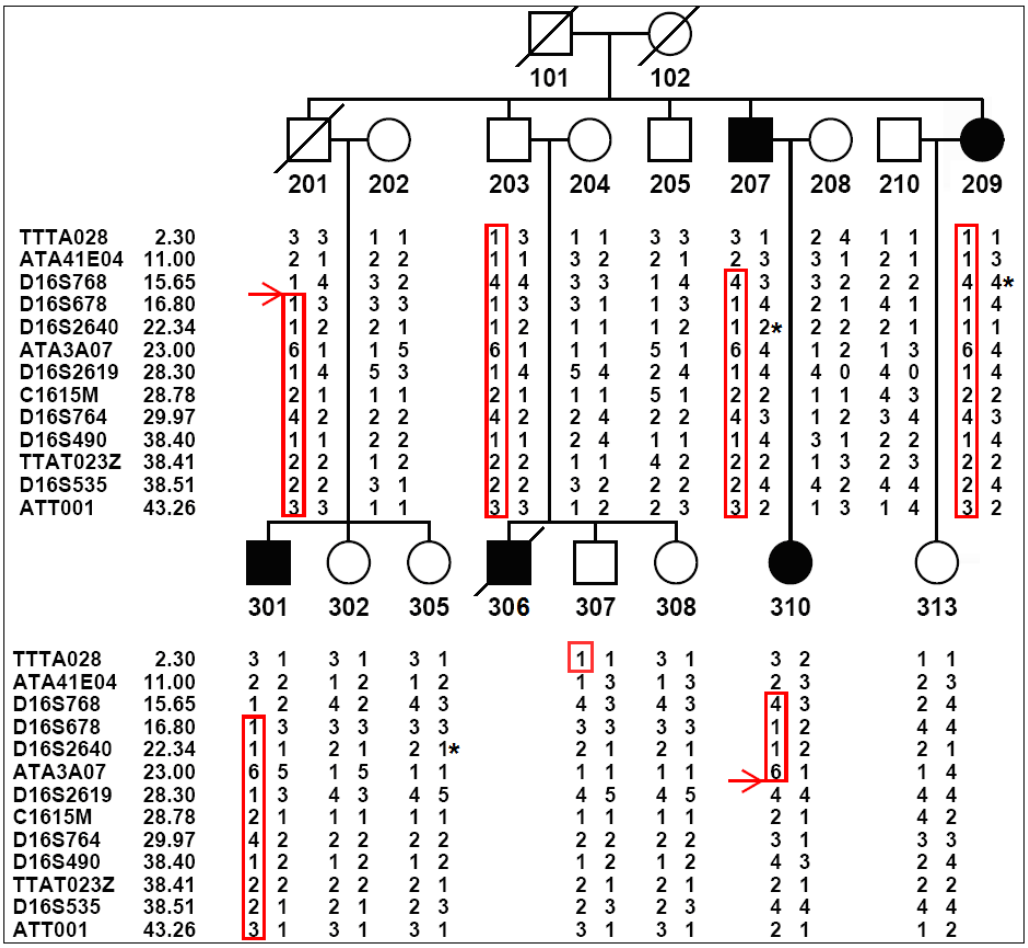

Figure 5.19. Haplotypes of HBT family at 16p13.3-p12.1. The haplotype harboring the disease locus is boxed, and the delimiting crossovers are shown with arrows. Possible mistypings identified by non-Mendelian error tests are indicated by asterisks.

6. DISCUSSION

6.1. FDH

We had initiated the genetic study in FHD family to identify the genetic locus for focal dermal hypoplasia. Inheritance for the disease had been well established as X-linked dominant (Goltz, 1992), which was in agreement with the pedigree of the family studied. Using this information, we focused on scanning the X-chromosome directly, rather than conducting a genome scan. Proof of linkage to X-chromosome was found in the early stages of the study. The FDH locus identified initially spanned 78 Mb, roughly half of the 153-Mb X-chromosome. Additional microsatellite markers were used for fine mapping this locus, seeking informative crossovers that would refine it. Eventually, using at least one marker at about every five million base pairs throughout this region (except in the immediate neighborhood of the centromere) and including all available members of the family, the locus was narrowed down to 52 Mb. It spanned roughly a third of the chromosome, including about a third of the genes encoded by the chromosome (489 out of 1529). The scarcity of crossovers in the family was surprising. We failed to spot a distinguishable candidate gene in this locus. Further application of candidate gene approach was not practical due to the sheer number of genes, causing the study to reach a dead end. At this stage, two reports were published that identified defects in PORCN, a protein functioning in the WNT signaling receptor pathway, as the underlying cause for FDH (Grzeschik *et al.,* 2007; Wang *et al.,* 2007). The first research group initially conducted linkage analysis in familial cases and obtained linkage to two loci on X-chromosome together covering 74 Mb. But the crucial advantage of access to a large number of unrelated FDH patients allowed further investigation. Both groups employed comparative genomic hybridization of genomic DNA samples from unrelated FDH patients and reference samples in search for genomic rearrangements. Both groups found X-chromosome deletions in several patients. Of the genes that resided in deleted regions, *PORCN* was the most probable candidate gene. Mutations in this gene were uncovered in other affected individuals by sequencing the exons and splice junctions.

In the light of those findings, we decided to analyze our patients for *PORCN* gene mutations. SSCP and DNA sequence analyses were carried out, first on exons with reported mutations, then on the rest of the coding sequences, and finally on the untranslated regions and the putative promoter. No mutation was detected. Initially DNA sequencing was to be used for confirmation and identification of SSCP pattern variations. SSCP analysis has a limited resolution, due to the lack of a universal optimum condition for resolving alleles. Thus, the lack of SSCP pattern variations were not taken as a conclusive result, and DNA sequence analysis was used for mutation screening for all fragments. Advances in sequencing technology and its widespread use have lowered service costs, allowing the wide use of this method.

Although the exons, splice sites and putative promoter of *PORCN* were devoid of mutations, the evidence that linked *PORCN* to FDH in the family came from qPCR experiment. Low levels of *PORCN* transcripts were observed in the two patients studied. The difference of reduction between the patients is probably caused by different levels of X-inactivation skewing, since reduction levels were correlated with phenotype severity.

Although no mutation was found, *PORCN* is still likely the gene responsible for this familial FDH. It is possible that a defect exists in other intronic or regulatory sequences, such as distal regulatory regions, explaining transcript level reduction. Other possibilities explaining the transcript level reduction in patients are copy number loss and splicing defects. Our assays could not rule out any genomic copy loss of *PORCN* resulting from a microdeletion. Sequenced amplicons did not uncover any SNPs to negate this possibility. Potential occurrence of splicing errors such as intron inclusion was not tested by checking transcript sizes of gene variants. Transcript level determination assays were limited in power due to the method used and the small sample size. Ascertainment of the current results can be achieved by using more powerful methods (qPCR experiments with oligonucleotide probes) and obtaining samples from additional patients. Since a correlation of X inactivation and phenotype severity has been previously proposed (Gorlin and Cohen 2001), assesment of X-inactivation skewing in our patients together with more conclusive expression data could provide information on the relation of *PORCN* expression and phenotype severity. A less likely possibility is that some other gene residing in the FDH locus may also be the cause for this case. The defects in this gene must account for the low

PORCN transcript levels, so it is expected to be a component of the WNT receptor signaling pathway, which may down-regulate *PORCN* when defected. Yet, none of the genes that reside in the FDH locus are known components of WNT receptor signaling pathway.

6.2. MHAC

The term autosomal recessive microhydranencephaly (MHAC) was designated to describe a phenotype detailed in Kavaslar *et al*. in 2000. Two affected brothers from a Slovak family presented a very similar phenotype. Rarity of the condition and occurrence in two siblings indicated hereditary basis, even in the face of no known parental consanguinity. This rare phenotype occurring in a second family immediately spawned the suspicion of an identical genetic cause in both families. Testing of this hypothesis proved negative. Slovak cases not linking to MHAC locus suggests locus heterogeneity for MHAC.

Pregnant mother of two patients in the Anatolian MHAC family requested a genetic diagnostic service. Determination of the genotype of the fetus was crucial, because the phenotype associated with MHAC is not detectable by MRI until late phases of the pregnancy. Homozygosity for the disease allele at the MHAC locus would have necessitated abortion, but luckily the fetus was found to be heterozygous, a healthy carrier. As the pregnancy concluded, the unaffected state of the newborn was confirmed.

The linkage studies for MHAC had been concluded and published by our research team previously. Later several genes residing at the MHAC locus had been analyzed as candidates, without finding any mutations. When we were contacted by a research group working on the new gene *C16ORF63*, we accepted their request to search for mutations in this gene. After completing gene analysis and failing to find any mutations, a search for other suitable candidates was initiated. A report linking pericentrin gene mutations to microcephaly (Rauch *et al.,* 2008) prompted us to reshape our criteria for candidate selection. As described earlier, *PLK1* and *NDE1* were assessed as the most likely candidates. PLK 1 is a serine/threonine kinase and a regulator of mitotic events. It was reported to localize to the kinetochores and to take part in the regulation of mitotic events

such as chromosome congression, chromosome segregation and cytokinesis. Most relevantly, it was reported to be required for proper spindle formation and function (Sumara *et al.,* 2004). NDE1 is a microtubule binding protein and a part of the mitotic spindle motor complex. Knockout mice for *NDE1* exhibited a small brain phenotype, which was suggested to result from mitotic spindle orientation anomalies (Feng *et al.,* 2004).

Analysis of *NDE1* and *PLK1* exons for sequence variations was continued in spite of the failure to amplify *NDE1* exon 2 from patient DNA. Repeated failures were attributed to a deletion in patients as the PCR amplification failure was specific to MHAC patients DNAs. Possibilities such as PCR optimization failure or an SNP at a primer binding site were ruled out.

We later identified the *NDE1* deletion in patients. It extended from intron 1 to intron 2, spanning 4275 bp and including exon 2. The deletion breakpoint regions were copies of a 56-bp repeat with 91 per cent homology and extending from 15 bp upstream to 41 bp downstream of each breakpoint. The deletion has thus resulted from an unequal inter- or intra-chromosomal recombination event at those highly similar sequences.

We propose that the 4275 base pair deletion of exon 2 and flanking sequences of *NDE1*, which resides in the well-established (LOD > 3) MHAC locus, is the causative mutation for MHAC phenotype in the Anatolian patients. The report that linked *NDE1* defects to small brain phenotype in mice (Feng *et al.,* 2004) has detailed the mechanism of action. NDE1 acts as a scaffold for formation of functional protein complexes at the microtubule organizing center during mitotic spindle assembly. This function is mediated by self interaction of NDE1 to form homodimers or homooligomers. Self interaction domain of NDE1 is the N terminal 91 amino acids. Through its scaffolding function, NDE1 regulates mitotic spindle orientation, which influences the cell fate. Disruption of NDE1 function leads to mitotic arrest. In the developmental stages of *NDE1* knockout mice, cortical neuron progenitors exit cell cycle and undergo premature cell differentiation. Frontal cortex development requires a healthy pool of progenitor cells, which migrate to upper layers of the cortex prior to differentiation. Reduction in the progenitor cell pool results in underdeveloped brain, hence the microcephaly phenotype.

The deletion in *NDE1* in MHAC patients removes exon 2, which includes the translation initiation codon and a part of the self association domain (amino acids 1-28). It is highly improbable that a functional gene product is produced in MHAC patients. This condition is similar to that in knockout mice, resulting in the small brain phenotype severely affecting the cerebral cortex. However, other features of the patients such as a small body size and hydranencephaly are not described in the mice. We attribute these phenotypic differences to species-specific differences between NDE1 orthologs. It has been reported that more than 20 per cent of the phenotypes due to null mutations in human and mouse ortholog genes may differ (Liao and Zhang, 2008). Similarity between mouse and human genes ranges from 70 per cent to 90 per cent, with *NDE1* gene products of mouse and human being 88 per cent similar. Also, tissue specific expression patterns may vary between the two species, as well as effects of other proteins on the *NDE1* null phenotype.

The proposal that the deletion in *NDE1* gene causes MHAC phenotype in Anatolian patients can be supported with further evidence. The lack of *NDE1* transcripts or functional protein product in MHAC patients could be evidenced. After this, the proposed mechanism of action can be supported if visualization of NDE1 - mitotic spindle co-localization in mitosis-induced cells from patients reveals significant increases in aberrant spindle formations.

6.3. HBT

The linkage study yielded strong evidence that the tumor development in the family studied had a hereditary basis. A lod score of 3.01 was observed at chromosome 16p13.2-p13.12, as well as a haplotype segregating with the disease. Although the lod score is above the criterion for accepting linkage, this result is not definitive because the actual penetrance is not known. Penetrance is definitely incomplete, since parents of two affected individuals are unaffected. The extent of penetrance can not be determined at this time, due to the impossibility of assigning any unaffected member as not carrying the disease gene. Considering the general low penetrance and late onset in cancer susceptibilities, there is the probability that any of the remaining 11 unaffected individuals who descended from the initial parents could have inherited the disease allele but not developed tumors. This

probability rendered impossible the elimination of some haplotypes shared by all patients and some unaffected members.

HBT locus spanned approximately 5.3 Mb and contained 54 genes. Candidate selection among those was done by using criteria based on association with tumor susceptibility and/or having tumor suppressor functions. Three genes in the minimal critical region were selected: *GSPT1*, *GRIN2A* and *SOCS1*. GSPT1 is a GTP binding protein, functioning in cell cycle control. It has been associated with gastric cancer susceptibility (Brito *et al.,* 2005). The glutamate receptor GRIN2A is reported to have tumor suppressor activity and is associated with colorectal carcinoma (Kim *et al.,* 2008). SOCS1 functions in immune response as a cytokine signaling inhibitor. This function suggested a tumor suppressor activity, and the gene was indeed found to be inactivated in hepatoblastomas (Nagai *et al.,* 2003) and silenced in myelomas (Galm *et al.,* 2003) and breast and ovary cancers (Sutherland *et al.,* 2004). Despite the fact that the linkage analysis did not yield conclusive information about the locus for this condition, in the lack of further information such as tumor formation in currently unaffected individuals, screening those three genes for defects in patients could lead to the identification of the genetic defect and thus the gene. This screening process was undertaken but not concluded due to low quality in DNA sequence analysis.

7. CONCLUSION

In the framework of this study, the causative gene for MHAC, *NDE1*, has been identified. Also, locus heterogeneity for MHAC has been revealed. Linkage of FDH to a locus on the X chromosome has been shown. Association of *PORCN* with the FDH cases were implied but no mutation on PORCN sequences was found. Lastly, a candidate locus for HBT has been identified.

REFERENCES

Alexander, I. E., G. P. Tauro and A. Bankier, "Fetal brain disruption sequence in sisters", *European Journal of Pediatrics,* Vol. 154 pp. 654-657, 1995.

Almeida, A., X. X. Zhu, N. Vogt, R. Tyagi, M. Muleris, A.M. Dutrillaux, B. Dutrillaux, D. Ross, B. Malfoy and S. Hanash, "GAC1, a new member of the leucine-rich repeat superfamily on chromosome band 1q32.1, is amplified and overexpressed in malignant gliomas", *Oncogene,* Vol. 16, pp. 2997-3002, 1998.

Behunova, J., E. Zavadilikova, T. M. Bozoglu, A. Gunduz, A. Tolun and C. Yalcinkaya., "Familial Microhydranencephaly Not Mapping to 16p13.13-12.2; Relation to Hereditary Fetal Brain Degeneration and Fetal Brain Disruption Sequence", *Clin Dysmorphol,* awaiting publication, 2008.

Brito, M., J. Malta-Vacas, B. Carmona, C. Aires, P. Costa, A. P. Martins, S. Ramos, A. R. Conde and C. Monteiro, "Polyglycine expansions in eRF3/GSPT1 are associated with gastric cancer susceptibility", *Carcinogenesis*, Vol. 12, 2046-2049, 2005.

Chernova, O. B., R. P. T. Somerville and J. K. Cowell, "A novel gene, LGI1, from 10q24 is rearranged and downregulated in malignant brain tumors", *Oncogene,* Vol. 17, pp. 2873-2881, 1998.

Engelke, D.R., A. Krikos, M. E. Bruck and D. Ginsburg, "Purification of Thermus aquaticus DNA polymerase expressed in Escherichia coli", *Anal. Biochem.,* Vol. 191, pp. 396–400, 1990.

Feng, Y. and C. A. Walsh, "Mitotic Spindle Regulation by Nde1 Controls Cerebral Cortical Size", *Neuron*, Vol. 44, pp. 279–293, 2004.

Fischer, U., D. Heckel, A. Michel, M. Janka, T. Hulsebos and E. Meese, "Cloning of a novel transcription factor-like gene amplified in human glioma including astrocytoma grade I", *Hum. Molec. Genet.,* Vol. 6, pp. 1817-1822, 1997.

Galm, O., H. Yoshikawa, M. Esteller, R. Osieka and J. G. Herman, "SOCS-1, a negative regulator of cytokine signaling, is frequently silenced by methylation in multiple myeloma", *Blood,* Vol. 101, pp. 2784-2788, 2003.

Goltz, R. W., W. C. Peterson Jr., R. J. Gorlin and H. G. Ravits, "Focal dermal hypoplasia"**,** *Archives of Dermatology,* Vol. 86, pp. 708-717, 1962.

Goltz, R. W., "Focal dermal hypoplasia syndrome: an update", *Archives of Dermatology,* Vol. 128, pp.1108-1111, 1992.

Gorlin, R.J., M. M. J. Cohen and R. C. M. Hennekam, "Syndromes of the Head and Neck", *Oxford Monographs on Medical Genetics,* Vol. 42, pp. 571–576, 2001.

Gorski, J. L., "Father-to-daughter transmission of focal dermal hypoplasia associated with nonrandom X-inactivation: support for X-linked inheritance and paternal X chromosome mosaicism", *Am. J. Med. Genet.,* Vol. 40, pp. 332-337, 1991.

Grzeschik, K. H., D. Bornholdt, F. Oeffner, A. Konig, M. del C. Boente, B. Fritz, M. Hertl, U. Grasshoff, K. Hofling, V. Oji, M. Paradisi, C. Schuchardt, Z. Szalai, G. Tadini, H. Traupe and R. Happle, "Deficiency of PORCN, a regulator of Wnt signaling, is associated with focal dermal hypoplasia", *Nature Genet.,* Vol. 39, pp. 833-835, 2007.

Henn, W., N. Blin and K. D. Zang, "Polysomy of chromosome 7 is correlated with overexpression of the erbB oncogene in human glioblastoma cell lines", *Hum. Genet.,* Vol. 74, pp. 104-106, 1986.

Kavaslar, G. N., S. Onengut, O. Derman, A. Kaya and A. Tolun, "The novel genetic disorder microhydranencephaly maps to chromosome 16p13.3-12.1", *American Journal of Human Genetics,* Vol. 66, pp. 1705-1709, 2000.

Kim, M.S., X. Chang, J. K. Nagpal, K. Yamashita, J. H. Baek, S. Dasgupta, G. Wu, M. Osada , J. H. Woo, W. H. Westra, B. Trink, E. A. Ratovitski, C. Moon and D. Sidransky, "The N-methyl-D-aspartate receptor type 2A is frequently methylated in human colorectal carcinoma and suppresses cell growth", *Oncogene*, Vol. 14, pp. 2045-2054, 2008.

Kinzler, K. W., S. H. Bigner, D. D. Bigner, J. M. Trent, M. L. Law, S. J. O'Brien, A. J. Wong and B. Vogelstein, "Identification of an amplified, highly expressed gene in a human glioma", *Science,* Vol. 236, pp. 70-73, 1987.

Lekanne Deprez, R. H., P. H. J. Riegman, N. A. Groen, U. L. Warringa, N. A. van Biezen, A. C. Molijn, D. Bootsma, P. J. de Jong, A. G. Menon, N. A. Kley, B. R. Seizinger and E. C. Zwarthoff, "Cloning and characterization of MN1, a gene from chromosome 22q11, which is disrupted by a balanced translocation in a meningioma", *Oncogene,* Vol. 10, pp. 1521-1528, 1995.

Liao, B. Y. and J. Zhang, "Null mutations in human and mouse orthologs frequently result in different phenotypes" *PNAS,* Vol. 105, pp. 6987-6992, 2008.

Lindner, T. H. and K. Hoffmann, "easyLINKAGE: A PERL script for easy and automated two-/multi-point linkage analyses", *Bioinformatics,* Vol. 21, pp. 405-407, 2005.

Nagai, H., T. Naka, Y. Terada, T. Komazaki, A. Yabe, E. Jin, O. Kawanami, T. Kishimoto, N. Konishi, M. Nakamura, Y. Kobayashi and M. Emi. "Hypermethylation associated with inactivation of the SOCS-1 gene, a JAK/STAT inhibitor, in human hepatoblastomas", *J. Hum. Genet.*, Vol. 48, pp. 65-69, 2003.

Rauch, A., C. T. Thiel, D. Schindler, U. Wick, Y. J. Crow, A. B. Ekici, A. J. van Essen, T. O. Goecke, L. Al-Gazali, K. H. Chrzanowska, C. Zweier, H. G. Brunner, K.

Becker, C. J. Curry, B. Dallapiccola, K. Devriendt, A. Dörfler, E. Kinning, A. Megarbane, P. Meinecke, R. K. Semple, S. Spranger, A. Toutain, R. C. Trembath, E. Voss, L. Wilson, R. Hennekam, F. de Zegher, H. G. Dörr and A. Reis, "Mutations in the pericentrin (PCNT) gene cause primordial dwarfism", *Science,* Vol. 319, pp. 816-819, 2008.

Reid, S., A. Renwick, S. Seal, L. Baskcomb, R. Barfoot, H. Jayatilake, The Breast Cancer Susceptibility Collaboration (UK); K. Pritchard-Jones, M. R. Stratton, A. Ridolfi-Luthy and N. Rahman, "Biallelic BRCA2 mutations are associated with multiple malignancies in childhood including familial Wilms tumour", *J. Med. Genet.,* Vol. 42, pp. 147-151, 2005.

Schram, A., H. Y. Kroes, K. Sollie, B. Timmer, P. Barth and T. van Essen, "Hereditary fetal brain degeneration resembling fetal brain disruption sequence in two sibships", *Am. J. Med. Genet.,* Vol. 127A, pp. 172-182, 2004.

Seven, M., Z. Suyugül, A. Yüksel, B. Geçkinli, S. Hacıhanefioğlu and A. Cenani, "A family representing goltz syndrome (focal dermal hypoplasia) in three generations", *The Turkish Journal of Pediatrics* Vol. 40, pp. 593-601, 1998.

Smith, J. S., I. Tachibana, U. Pohl, H. K. Lee, U. Thanarajasingam, B. P. Portier, K. Ueki, S. Ramaswamy, S. J. Billings, H. W. Mohrenweiser, D. N. Louis and R. B. Jenkins, "A transcript map of the chromosome 19q-arm glioma tumor suppressor region", *Genomics,* Vol. 64, pp. 44-50, 2000.

Staal, F. J. T., R. B. van der Luijt, M. R. M. Baert, J. van Drunen, H. van Bakel, E. Peters, I. de Valk, H. K. P. van Amstel, M. J. B. Taphoorn, G. H. Jansen, C. W. M. van Veelen, B. Burgering and G. E. J. Staal, "A novel germline mutation of PTEN associated with brain tumours of multiple lineages", *Brit. J. Cancer,* Vol. 86, pp. 1586-1591, 2002.

Sumara, I., J. F. Gimenez-Abian, D. Gerlich, T. Hirota, C. Kraft, C. de la Torre, J. Ellenberg and J. M. Peters, "Roles of Polo-like Kinase 1 in the Assembly of Functional Mitotic Spindles", *Current Biology*, Vol. 14, pp. 1712–1722, 2004.

Sutherland, K. D., G. J. Lindeman, D. Y. Choong, S. Wittlin, L. Brentzell, W. Phillips, I. G. Campbell and J. E. Visvader, "Differential hypermethylation of SOCS genes in ovarian and breast carcinomas", *Oncogene*, Vol. 23, pp. 7726-7733, 2004.

Tura, A., "Analysis of the locus for microhydranencephaly", M. S. Thesis, Boğaziçi University, 2001.

Wang, X., V. R. Sutton, J. O. Peraza-Llanes, Z. Yu, R. Rosetta, Y.C. Kou, T. N. Eble, A. Patel, C. Thaller, P. Fang and I. B. Van den Veyver, "Mutations in X-linked PORCN, a putative regulator of Wnt signaling, cause focal dermal hypoplasia", *Nature Genet.,* Vol. 39, pp. 836-838, 2007.

Weber, J.L. and K. W. Broman, "Genotyping for human whole-genome scans: Past, present, and future", *Adv. Genet.,* Vol. 42, pp. 77-96, 2001.

Wellenreuther, R., J. A. Kraus, D. Lenartz, A. G. Menon, J. Schramm, D. N. Louis, V. Ramesh, J. F. Gusella, O. D. Wiestler and A. von Deimling, "Analysis of the neurofibromatosis gene reveals molecular variants of meningioma", *Am. J. Path.,* Vol. 146, pp. 827-832, 1995.

Zhou, X.-P., W. M. Smith, O. Gimm, E. Mueller, X. Gao, P. Sarraf, T. W. Prior, C. Plass, A. van Deimling, P. M. Black, A. J. Yates and C. Eng, "Over-representation of PPAR-gamma sequence variants in sporadic cases of glioblastoma multiforme: preliminary evidence for common low penetrance modifiers for brain tumour risk in the general population", *J. Med. Genet.,* Vol. 37, pp. 410-414, 2000.